

MAGNETOSPHERES OF " HOT JUPITERS ": THE IMPORTANCE OF MAGNETODISKS IN SHAPING A MAGNETOSPHERIC OBSTACLE

M. L. Khodachenko, I Alexeev, E Belenkaya, H Lammer, Jean-Mathias Griessmeier, M Leitzinger, P Odert, T Zaqarashvili, H.O. Rucker

▶ **To cite this version:**

M. L. Khodachenko, I Alexeev, E Belenkaya, H Lammer, Jean-Mathias Griessmeier, et al.. MAGNETOSPHERES OF " HOT JUPITERS ": THE IMPORTANCE OF MAGNETODISKS IN SHAPING A MAGNETOSPHERIC OBSTACLE. The Astrophysical Journal, 2012, 744 (70), 16 p. 10.1088/0004-637X/744/1/70 . insu-01351029

HAL Id: insu-01351029
https://insu.hal.science/insu-01351029

Submitted on 21 Sep 2016

HAL is a multi-disciplinary open access archive for the deposit and dissemination of scientific research documents, whether they are published or not. The documents may come from teaching and research institutions in France or abroad, or from public or private research centers.

L'archive ouverte pluridisciplinaire **HAL**, est destinée au dépôt et à la diffusion de documents scientifiques de niveau recherche, publiés ou non, émanant des établissements d'enseignement et de recherche français ou étrangers, des laboratoires publics ou privés.



Distributed under a Creative Commons Attribution - NonCommercial - NoDerivatives 4.0 International License

The Astrophysical Journal, 744:70 (16pp), 2012 January 1 doi:10.1088/0004-637X/744/1/70
© 2012. The American Astronomical Society. All rights reserved. Printed in the U.S.A.

MAGNETOSPHERES OF "HOT JUPITERS": THE IMPORTANCE OF MAGNETODISKS IN SHAPING A MAGNETOSPHERIC OBSTACLE

M. L. Khodachenko[1], I. Alexeev[2], E. Belenkaya[2], H. Lammer[1], J.-M. Grießmeier[3], M. Leitzinger[4], P. Odert[4], T. Zaqarashvili[1], and H. O. Rucker[1]

[1] Space Research Institute, Austrian Academy of Sciences, Graz A-8042, Austria; maxim.khodachenko@oeaw.ac.at, helmut.lammer@oeaw.ac.at
[2] Skobeltsyn Institute of Nuclear Physics, Lomonosov Moscow State University, Moscow 119992, Russia; alexeev@dec1.sinp.msu.ru
[3] Laboratoire de Physique et Chimie de l'Environnement et de l'Espace, Orleans 45071, France; jean-mathias.griessmeier@cnrs-orleans.fr
[4] Institute for Physics, IGAM, Karl-Franzens-University, Graz A-8010, Austria; martin.leitzinger@uni-graz.at, petra.odert@uni-graz.at
Received 2010 October 6; accepted 2011 September 12; published 2011 December 14

ABSTRACT

Weak intrinsic magnetic dipole moments of tidally locked close-in giant exoplanets ("hot Jupiters") have been shown in previous studies to be unable to provide an efficient magnetospheric protection for their expanding upper atmospheres against the stellar plasma flow, which should lead to significant non-thermal atmosphere mass loss. The present work provides a more complete view of the magnetosphere structure of "hot Jupiters," based on a paraboloid magnetospheric model (PMM). Besides the intrinsic planetary magnetic dipole, the PMM considers among the main magnetic field sources also the electric current system of the magnetotail, magnetopause currents, and the ring current of a magnetodisk. Due to the outflow of ionized particles from the hydrodynamically expanding upper atmosphere, "hot Jupiters" may have extended magnetodisks. The magnetic field produced by magnetodisk ring currents dominates above the contribution of an intrinsic magnetic dipole of a "hot Jupiter" and finally determines the size and shape of the whole magnetosphere. A slower-than-the-dipole-type decrease of the magnetic field with the distance forms the essential specifics of magnetodisk-dominated magnetospheres of "hot Jupiters." This results in their 40%–70% larger scales compared to those traditionally estimated by only the planetary dipole taken into account. Therefore, the formation of magnetodisks has to be included in the studies of the stellar wind plasma interaction with close-in exoplanets, as well as magnetospheric protection for planetary atmospheres against non-thermal escape due to erosion by the stellar plasma flow.

Key words: planets and satellites: magnetic fields – planets and satellites: physical evolution – planets and satellites: rings – planet–star interactions

1. INTRODUCTION

The questions regarding evolutionary paths of exoplanets and their key influencing factors nowadays are the subject of continuous attention in the scientific community. Among these questions, a prominent position belongs to the problem of stellar–planetary interactions, including consideration of influence of stellar radiation and plasma flows, e.g., stellar winds and coronal mass ejections (CMEs), on planetary environments and evolution of exoplanets (Lammer et al. 2003, 2007; Erkaev et al. 2005; Khodachenko et al. 2007b, 2007a). Magnetic fields, those connected with the planetary intrinsic magnetic dipole moment $\mathcal{M}$, as well as the magnetic fields associated with electric current systems induced in close planetary plasma surroundings play an important role here. They form a planetary magnetosphere which acts as an obstacle (magnetospheric obstacle), interacting with the stellar wind. This magnetospheric obstacle protects planetary ionospheres, upper atmospheres, and in the case of terrestrial planets—the surfaces—against the direct impact of stellar plasmas and energetic particles (e.g., cosmic rays).

This paper concentrates on peculiarities of giant exoplanet magnetospheres. At the same time, the major approaches and views presented here may also be converted to the cases of smaller rocky exoplanets taking into account their specific features and appropriate physics. The family of known giant exoplanets can be subdivided into two main groups: (1) rather short orbit (in other words "close-in") Jupiter-type planets, with an orbital distance $d < 0.3$ AU—the so-called hot Jupiters; and (2) a bit more massive giant planets at larger orbital distances $d \geqslant 1$ AU. The latter also include ice giants located at $d > 10$ AU. By this, the close-in "hot Jupiters" represent a rather substantial fraction, of about 30%, of all presently known exoplanets.

The upper atmospheres of close-in "hot Jupiters," heated by the stellar X-ray/EUV (XUV) radiation and exposed to stellar wind plasma flows, undergo thermal (due to hydrodynamic expansion; Lammer et al. 2003; Baraffe et al. 2004; Grießmeier et al. 2004; Yelle 2004, 2006; Tian et al. 2005; Penz et al. 2008; Lammer et al. 2009) and non-thermal (due to a direct interaction with the stellar wind plasmas; Erkaev et al. 2005; Khodachenko et al. 2007a; Lammer et al. 2009) mass loss. The closer an exoplanet is to its host star, the more efficient are these processes, and therefore, the more important becomes the magnetospheric protection of the planet. Hydrodynamic expansion of a planetary upper atmosphere, heated by stellar XUV flux, with the resulting photoionization of the expanding atmospheric gas leads to the formation of an extended, essentially dynamical ionosphere/plasmasphere (Koskinen et al. 2010). The interaction of such expanding planetary plasma envelopes with the stellar winds and the intrinsic planetary magnetic fields leads to the development of a new type of magnetospheres, not typical for the solar system planets. The effect of an expanding planetary upper ionosphere has been studied for a non-magnetized terrestrial-type exoplanet numerically in Johansson et al. (2009). Besides that, recently Trammell et al. (2011) have analyzed the internal structure of a "hot Jupiter" magnetosphere, paying attention to the specifics of the internal magnetic field configuration and plasma dynamics, but ignoring the interaction of the planetary magnetic obstacle with a stellar wind. The present

work makes a step forward in that study and provides a more complete view of a "hot Jupiter" magnetosphere structure and topology. We pay attention to the fact that during the significant thermal outflow of atmospheric gas of close-in "hot Jupiters," the upper layers of the expanding planetary atmospheres, ionized by stellar radiation, contribute to the formation of extended current-carrying plasma disks around the planets. By this, the rotation of the planet and the presence of even a small intrinsic magnetic dipole moment play a crucial role in the formation of the disk. The electric currents induced in the plasma disk produce an essential effect on the overall magnetic field structure around the planet, resulting in the formation of a *magnetodisk-dominated magnetosphere* of a close-in "hot Jupiter." Due to the certain extension of the plasma disks around close-in exoplanets, the sizes of their magnetodisk-dominated magnetospheres are usually larger than those followed from the traditional estimations based on the account of only the screened planetary magnetic dipoles (Grießmeier et al. 2004; Khodachenko et al. 2007a).

The structure of an exoplanet magnetosphere depends also on a speed regime of the stellar wind plasma relative to the planet (Erkaev et al. 2005; Ip et al. 2004; Grießmeier et al. 2007a). In the case of an extremely close orbital location of an exoplanet (e.g., $d < 0.03$ AU for the Sun-analog star), where the stellar wind is still under acceleration and remains not very fast ($v_{sw} < 200$ km s^{-1}), but hot ($T \sim 10^6$ K), dense ($n_{sw} > 10^4$ cm^{-3}), and with a relatively high ambient magnetic field ($B > 10^{-2}$ G) (Ip et al. 2004; Erkaev et al. 2005; Preusse et al. 2005; Lammer et al. 2009), the relative speed $\tilde{v}_{sw}$ between an exoplanet and stellar wind plasma may be submagnetosonic and sub-Alfvénic. This would result in the absence of a bow shock in the upstream region leading to the formation of an Alfvénic wing-type magnetosphere. The present paper, however, does not consider such cases, aiming at moderately short orbit giant planets (0.3 AU $\geqslant d \geqslant$ 0.045 AU) near solar-type stars, under the conditions of a super-Alfvénic stellar wind flow, i.e., with the magnetospheres having in a general case a bow shock, a magnetopause, a magnetotail, and a magnetodisk.

The magnetosphere of a "hot Jupiter" is a complex object, whose formation and evolution depend on different external and internal factors. These factors may be subdivided into two basic groups: (1) *stellar factors*, e.g., stellar activity, radiation, and stellar plasma flow (stellar wind, CMEs); and (2) *planetary factors*, e.g., orbital characteristics, planetary magnetic field, and mass loss. In particular, the key magnetosphere influencing parameters, which we take into consideration in this work, are the parameters of the stellar wind (density n_{sw} and velocity v_{sw}), angular velocity of planetary rotation ω_p, the value of the planetary intrinsic magnetic dipole moment $\mathcal{M}$, and the rate of mass load to the magnetodisk, controlled by the planetary thermal mass loss $dM_p^{(th)}/dt$. The latter depends on the stellar activity and XUV radiation. Therefore, in the next sections, before the modeling of a "hot Jupiter" magnetosphere, we briefly address these key input parameters and provide their typical values.

A semi-analytical approach to the modeling of a "hot Jupiter" magnetosphere structure is applied. It is based on a paraboloid magnetospheric model (PMM) developed in Alexeev & Shabansky (1972), Alexeev (1978, 1986), Alexeev & Bobrovnikov (1997), and Alexeev et al. (2003). Besides the intrinsic planetary magnetic dipole and magnetopause currents, the PMM has among the main sources of the magnetic field also the electric current system of the magnetotail and the induced ring currents of the magnetodisk. The model works without any restrictions imposed on the values of interplanetary medium parameters. It enables the description of the whole variety of possible magnetosphere configurations caused by different intrinsic magnetic fields of exoplanets and various stellar wind conditions. The key matter of this paper is the application of the PMM to a hypothetical extrasolar gas giant with the size and mass of the solar system Jupiter (e.g., $M_p = 1.0\,M_J = 1.89 \times 10^{27}$ kg, $r_p = 1.0\,R_J = 71.5 \times 10^3$ km), located at different orbital distances around a 4 Gyr old solar-analog G-type star ($M_* = 1.0\,M_{Sun} = 1.99 \times 10^{30}$ kg, $R_* = 1.0\,R_{Sun} = 69.6 \times 10^4$ km).

The paper is organized in the following way. In Section 2 we provide estimations of the stellar wind plasma flow parameters at different orbital distances from a star. Section 3 discusses the properties of an intrinsic magnetic dipole of a close-in giant exoplanet, taking into account the effect of tidal locking, and addresses the problem of planetary magnetospheric protection. Section 4 deals with an estimation of the thermal mass loss of an upper atmosphere of a close-in gas giant exoplanet heated by stellar XUV radiation. In Section 5, based on the inputs from Sections 2, 3, and 4, a PMM approach to the modeling of the magnetosphere of a close-in "hot Jupiter" with a magnetodisk is introduced, and the estimations of typical values of the exoplanetary magnetosphere size (magnetopause stand-off distance) are provided. Section 6 discusses the issues of the "hot Jupiter" magnetospheric protection and the importance of a magnetodisk in that respect. The Appendix gives additional details regarding the PMM.

2. STELLAR WIND PLASMA FLOW

Stellar wind plasma flow impacts the planetary environment and influences the size, shape, and dynamics of the planetary magnetospheric obstacle. The density n_{sw} and relative velocity $\tilde{v}_{sw}$ of the stellar wind encountered by a planet are the key parameters which determine the size and shape of the magnetosphere. For the small orbital distances ($d < 0.3$ AU) relevant for "hot Jupiters" at approximately circular orbits, the orbital velocity of a planet given by Kepler's law $V_K = d\Omega$ is approximately perpendicular to the stellar wind velocity v_{sw} in the reference system of the star. Here $\Omega = \sqrt{M_* G/d^3}$ is the orbital angular velocity of a planet, where G is the gravitational constant and M_* is the mass of the star. Therefore, the relative speed between an exoplanet and stellar wind plasma can be estimated as $\tilde{v}_{sw} = \sqrt{V_K^2 + v_{sw}^2}$. In view of that, in the case of close-in exoplanets $\tilde{v}_{sw}$ may differ considerably from v_{sw} (Grießmeier et al. 2007a). Since n_{sw} and v_{sw} vary with the stellar age and depend also on the stellar spectral type, as well as on the orbital distance of the planet, the efficiency of magnetospheric protection for similar planets orbiting different stars at different orbits will be different and it will change also in course of evolution of the star and the planet.

Currently good knowledge exists of n_{sw} and v_{sw} for the Sun, whereas the amount of corresponding data related to other stars is much more limited. While the dense stellar winds from hot stars, cool giants/supergiants, and young T Tauri stars produce detectable spectroscopic features from which the wind parameters can be derived, the tenuous winds from Sun-like G-type stars are several orders of magnitude less massive and cannot be detected spectroscopically. Recently, there have been important developments toward indirect detections of stellar winds through their interactions with the surrounding

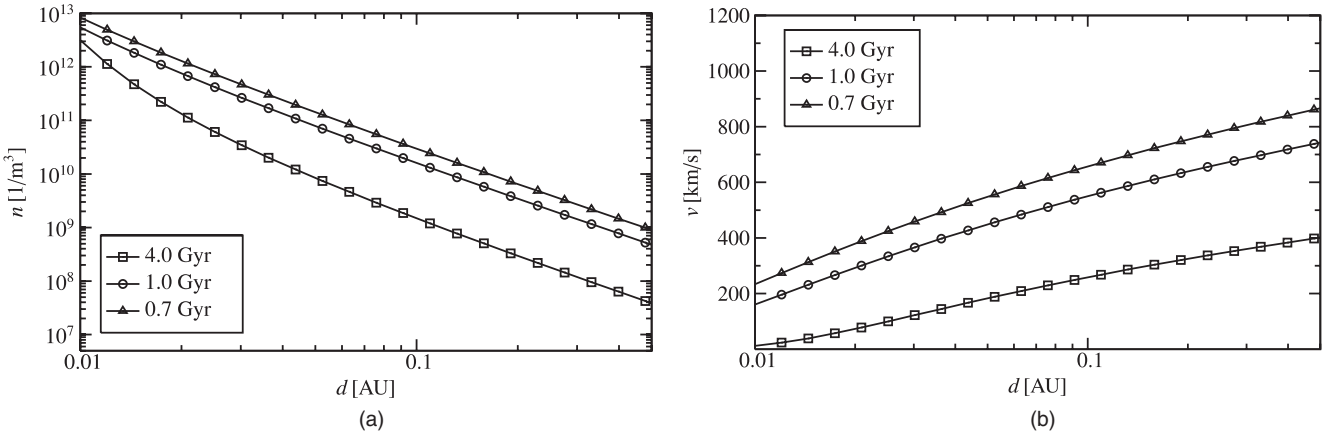


Figure 1. Stellar wind density (a) and velocity (b) change with distance from a solar-analog G-type star of different ages: 0.7, 1, and 4 Gyr.

interstellar medium. In particular, the stellar mass-loss rates and related stellar wind parameters have been estimated by using the *Hubble Space Telescope* high-resolution measurements of the characteristic Lyman-α absorption feature at 1216 Å (created by neutral hydrogen at the astropause), associated with the interaction between the fully ionized stellar coronal winds and the partially ionized local interstellar medium (Wood et al. 2002, 2005).

Combining the stellar mass-loss measurements of Wood et al. (2005) with the results of Newkirk (1980) for the age dependence of stellar wind velocity, Grießmeier et al. (2007a) estimated the time dependence of the stellar wind velocity and density at 1 AU (e.g., $n_{\rm sw}(t, d = 1\,{\rm AU})$ and $v_{\rm sw}(t, d = 1\,{\rm AU})$) and proposed a method for the calculation of the stellar wind density $n_{\rm sw}(t_*, d, M_*, R_*)$ and velocity $v_{\rm sw}(t_*, d, M_*, R_*)$ at a given orbital location of an exoplanet d for a given mass M_*, radius R_*, and age t_* of a star. According to Grießmeier et al. (2007a), the radial dependence of the stellar wind properties for stellar ages >0.7 Gyr can be described by a Parker-type (Parker 1958) stellar wind model. In this model, the interplay between stellar gravitation and pressure gradients leads to a supersonic gas flow formed at sufficiently large distances from a star. The free parameters of the model are the coronal temperature $T_{\rm corona}$ and the stellar mass-loss rate $\dot{M}_*$, which similarly to Mann et al. (1999) are defined by adjusting the Parker model solution to the stellar wind velocity value $v_{\rm sw}(t_*, d = 1\,{\rm AU})$ at 1 AU given for a prescribed stellar system age t_*. For details of this procedure see Grießmeier et al. (2005, 2007a, 2009). An example of such a result is demonstrated in Figure 1, which shows the dependence of $n_{\rm sw}$ and $v_{\rm sw}$ on the distance from a solar-analog G-type star of different ages: 0.7; 1; 4 Gyr. The isothermal Parker model has been used for these calculations. In spite of containing a strong idealization assumption (constant temperature of the wind $T_{\rm sw}$), the model is known to reproduce well the results of more complicated stellar wind models at the relatively short orbital distances ($d \leqslant 0.3$ AU) considered in the present paper.

For the practical needs of a "hot Jupiter" magnetosphere model, Table 1 summarizes the values of stellar wind plasma parameters for a solar-analog G-type star ($M_* = M_{\rm Sun}$, age: 4 Gyr) at orbital distances of 0.045 AU, 0.1 AU, and 0.3 AU. Note that the provided values for $\tilde{v}_{\rm sw}$ in Table 1 correspond to the relative velocity of the stellar wind plasma with respect to a planet, i.e., they include also the orbital velocity of a planet V_K, as defined above in this section.

It is worth noting that exoplanets at close orbital locations $\lesssim$0.3 AU to their host stars may also experience strong impacts

Table 1
Stellar Wind Plasma Parameters for a Solar-analog G-type Star ($M_* = M_{\rm Sun}$, Age: 4 Gyr) at Different Orbital Distances d

d (AU)	$n_{\rm sw}$ (cm^{-3})	$\tilde{v}_{\rm sw}$ (km s^{-1})
0.045	9.1×10^3	210
0.1	1.2×10^3	260
0.3	92	340

Note. The values of stellar wind velocity $\tilde{v}_{\rm sw}$ include a contribution of the corresponding Keplerian planetary orbital velocity V_K.

of the stellar CMEs. By considering the Sun as a typical representative of G-type stars, it seems reasonable to assume a similarity of the stellar CME activity of G-type stars to that known for the Sun. Khodachenko et al. (2007b) have shown that for a critical CME production rate of ≈36 CMEs per day (and higher) a close orbit exoplanet appears under continuous action of stellar CMEs, so that each next CME collides with the planet during the time when the previous CME is still passing over it. Under the conditions of continuous CME flow acting on a planet, the parameters of the stellar wind ($n_{\rm sw}$, $\tilde{v}_{\rm sw}$, etc.) have to be replaced by the corresponding parameters of CME plasma (Khodachenko et al. 2007b); that means the harder conditions for the planetary environments than those existing in the case of a regular stellar wind. This may have crucial consequences for the type and size of magnetospheres of close-in exoplanets near the flaring stars. However, this topic deserves a separate study. That is beyond the scope of the present paper.

3. INTRINSIC MAGNETIC FIELDS OF "HOT JUPITERS" AND THE PROBLEM OF MAGNETOSPHERIC PROTECTION OF EXOPLANETS

An intrinsic magnetic field of a planet, which influences the character of the magnetospheric obstacle, is generated by a magnetic dynamo. The existence and efficiency of the dynamo are closely related to the type of the planet and its interior structure. Not all planets have intrinsic magnetic fields, or in other words, efficiently operating dynamos. Planetary magnetic dynamo requires the presence of an electrically conducting region (i.e., a liquid outer core for terrestrial planets, or a layer of electrically conducting liquid hydrogen for gas giants) with non-uniform flows organized in a certain manner, which create a self-sustaining magnetic field. According to dynamo theory, this flow should be convective in nature (Stevenson 1983). Therefore,

convection can be regarded as a necessary requirement for a planetary magnetic field (Stevenson 2003).

Limitations of the existing observational techniques make direct measurements of the magnetic fields of exoplanets impossible. At the same time, a rough estimation of an intrinsic planetary magnetic dipole moment $\mathcal{M}$ can be obtained by simple scaling laws found by the comparison of different contributions in the governing equations of planetary magnetic dynamo theory (Farrell et al. 1999; Sánchez-Lavega 2004; Grießmeier et al. 2004; Christensen 2010). Most of these scaling laws reveal a connection between the intrinsic magnetic field and rotation of a planet. More recently, Reiners & Christensen (2010), based on scaling properties of convection-driven dynamos (Christensen & Aubert 2006), have calculated the evolution of average magnetic fields of "hot Jupiters" and found that (1) extrasolar gas giants may start their evolution with rather high intrinsic magnetic fields, which then decrease during the planet life time; and (2) the planetary magnetic moment may be independent of planetary rotation (Reiners & Christensen 2010). In the present work we focus on the structure of giant exoplanet magnetospheres and do not consider the long time evolution of the planetary magnetic fields. Therefore, below we proceed with the approach of Grießmeier et al. (2004, 2005, 2007a), who estimated the intrinsic planetary magnetic dipole moments of exoplanets and corresponding sizes of their magnetospheres using the following scaling laws for $\mathcal{M}$:

$$\begin{aligned}
&\mathcal{M} \propto \rho_c^{1/2}\omega_p r_c^4 && \text{(Busse 1976)},\\
&\mathcal{M} \propto \rho_c^{1/2}\omega_p^{1/2} r_c^3 \sigma^{-1/2} && \text{(Stevenson 1983)},\\
&\mathcal{M} \propto \rho_c^{1/2}\omega_p^{3/4} r_c^{7/2} \sigma^{-1/4} && \text{(Mizutani et al. 1992)},\\
&\mathcal{M} \propto \rho_c^{1/2}\omega_p r_c^{7/2} && \text{(Sano 1993)}.
\end{aligned} \tag{1}$$

Here r_c is the radius of the dynamo region (also called the core radius) and ω_p is the angular velocity of a planet rotation around its axis. The internal properties of a planet such as the mass density and the conductivity of the dynamo region are denoted by ρ_c and σ, respectively (for details of the model parameter estimation see Grießmeier et al. 2004, 2007b).

Equations (1) provide a range $\mathcal{M}_{\min} - \mathcal{M}_{\max}$ of reasonable planetary magnetic moment values. In spite of being different in details, all of these models yield an increase of $\mathcal{M}$ with an increasing planetary angular velocity ω_p. In that respect it is necessary to take into account the fact that close-in exoplanets such as "hot Jupiters" very likely are tidally locked to their host stars. The angular rotation of a tidally locked planet is synchronized with its orbital motion so that ω_p is equal to the orbital angular velocity Ω determined by Kepler's law. The timescale for tidal locking τ_{sync} depends on the planetary structure, orbital distance to the host star, and the stellar mass (Showman & Guillot 2002). By this, the planets for which $\tau_{sync} \leqslant 0.1$ Gyr can be assumed to be tidally locked, since the age of a planet is at least an order of magnitude longer. On the other hand, the planets with $\tau_{sync} \geqslant 10$ Gyr are almost certainly tidally unlocked. The general trend is that the closer planetary orbit is to the host star, the shorter is τ_{sync}. The influence of tidal locking on the value of an expected planetary magnetic dipole was studied for different planets (giants and terrestrial type) in Sánchez-Lavega (2004) and Grießmeier et al. (2004, 2007b). It was shown that the magnetic moments of slowly rotating tidally locked exoplanets are usually much smaller than those for similar but freely rotating tidally unlocked planets. This can also be seen in Figure 2, which shows the range of possible

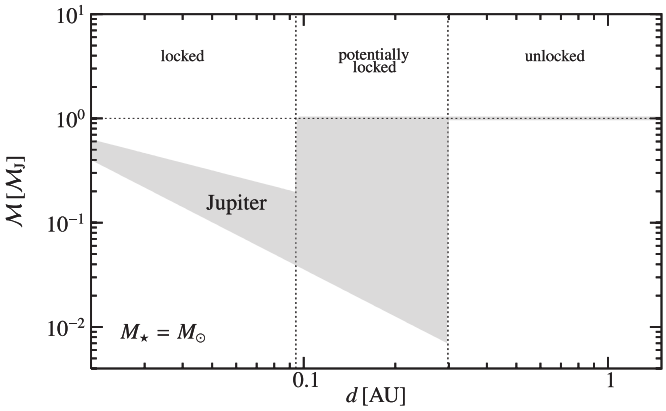


Figure 2. Range of possible magnetic moments defined by Equation (1) for a Jupiter-type ($M_p = M_J$; $r_p = R_J$) giant exoplanet, orbiting around a solar-analog ($M_* = M_{Sun}$, $R_* = R_{Sun}$) G-type star. Tidal locking causes a significant decrease of the magnetic moments of the close-in planets compared to the unlocked freely rotating ones.

planetary magnetic dipole moments defined by Equation (1) for a Jupiter-type ($M_p = M_J$; $r_p = R_J$) exoplanet orbiting around a solar-analog G-type star ($M_* = M_{Sun}$, $R_* = R_{Sun}$). The values of $\mathcal{M}$ are scaled in units of the present time Jupiter magnetic moment $\mathcal{M}_J = 1.56 \times 10^{27}$ A m^2.

The size of the planetary magnetic obstacle (e.g., magnetosphere) is characterized by the magnetopause substellar standoff distance R_s. It is defined from the balance between the stellar wind kinetic ram pressure and the planetary magnetic field pressure at the substellar point (Baumjohann & Treumann 1997; Grießmeier et al. 2004, 2007a; Khodachenko et al. 2007b; Durand-Manterola 2009). The value of an intrinsic magnetic dipole moment $\mathcal{M}$ plays an important role in defining the size and shape of the planetary magnetosphere, and therefore the magnetospheric protection of a planet. So far, the investigations of planetary magnetospheric protection were made within a highly simplifying assumption of a *planetary dipole-dominated magnetosphere*. This means that only the intrinsic magnetic dipole moment of an exoplanet and the corresponding magnetopause electric currents have been considered as the major magnetosphere forming factors (Grießmeier et al. 2004; Khodachenko et al. 2007a, 2007b; Holmström et al. 2008; Ekenbäck et al. 2010). In this case, i.e., assuming $B(r) \propto \mathcal{M}/r^3$, the value of R_s has been defined by the following expression (Baumjohann & Treumann 1997):

$$R_s \equiv R_s^{(dip)} = \left[\frac{\mu_0 f_0^2 \mathcal{M}^2}{8\pi^2 \rho_{sw} \tilde{v}_{sw}^2}\right]^{1/6}, \tag{2}$$

where μ_0 is the diamagnetic permeability of free space, $f_0 \approx 1.22$ is a form factor of the magnetosphere caused by the account of the magnetopause electric currents, $\rho_{sw} = n_{sw} m$ is the mass density of the stellar wind, and $\tilde{v}_{sw}$ is the relative velocity of the stellar wind plasma which includes also the planetary orbital rotation velocity.

In general there are other terms which might be important in the pressure balance, but were not taken into account in the course of obtaining Equation (2). These are, in particular, the magnetic pressure of the interplanetary magnetic field (IMF) and plasma pressure inside the magnetosphere. The inclusion of IMF may be important for the pressure balance in the substellar magnetosphere point under certain circumstances. However, in the present study we consider the case of a super-Alfvénic flow of the stellar wind encountered by an exoplanet

Table 2
Ranges of $\mathcal{M}$ Given by Equation (1) and $R_s = R_s^{(dip)}$ Provided by Equation (2) for a Jupiter-type Exoplanet Orbiting a Solar-analog G-type Star at Different Distances d under the Action of the Stellar Wind Plasma Flow Described in Table 1

d (AU)	$\mathcal{M}$ ($\mathcal{M}_J$)	$R_s^{(dip)}(\mathcal{M}_{min})/R_s^{(dip)}(\mathcal{M}_{max})$ (r_p)
0.045[a]	0.12–0.3	4.3–6.2
0.1[b]	0.04–1.0	3.8–12
0.3[c]	1.0–1.0	15–15

Notes.
[a] Tidally locked.
[b] Possible tidally locked.
[c] Not tidally locked.

located outside of the stellar Alfvénic sphere. This means that $\tilde{v}_{sw} > V_A$, and the dynamic pressure of stellar wind plasma dominates above the IMF pressure. As to the pressure of plasma inside magnetosphere, below (in Section 5.3) we take it into account as the pressure of magnetodisk plasma p_{mp}. The analysis of Equations (10) and (11) there shows that within the adopted approach, the contribution of plasma pressure to the total pressure balance in the substellar point is about 17% of the magnetic field pressure produced by the current systems of the magnetodisk and the corresponding magnetopause currents.

For the tidally locked close-in exoplanets with weak magnetic moments exposed to a dense and/or fast stellar wind plasma flows, Equation (2) yields rather small values for R_s, which in the most extreme cases may even shrink down to the planetary radius r_p (Khodachenko et al. 2007a). Table 2 provides the ranges for $\mathcal{M}$ obtained with Equation (1), as well as the values of the dipole-dominated magnetopause stand-off distance $R_s^{(dip)}$ given by Equation (2) for a Jupiter-type giant exoplanet orbiting around a solar-analog G-type star at different distances (0.045; 0.1; 0.3 AU) and appearing under the action of the stellar wind, characterized by the parameters as given in Table 1. The values of $R_s^{(dip)}$ are given in units of the Jovian radius $r_p \equiv R_J$.

As can be seen from Table 2, small values of intrinsic magnetic moments of tidally locked close-in "hot Jupiters" result in rather small sizes of dipole-dominated magnetospheres, $R_s = R_s^{(dip)}$, compressed by the stellar wind down to only several planetary radii. Such small magnetospheres have been shown to be unable to provide efficient protection of planetary upper atmospheres against strong non-thermal mass loss, essential at short orbital distances from the stars (Khodachenko et al. 2007b, 2007a; Lammer et al. 2007, 2009). The estimates of the non-thermal mass loss of magnetically unprotected "hot Jupiters," due to the stellar wind ion pickup, lead to significant and sometimes unrealistic values—up to several tens of planetary masses M_p lost during a planet's life time (Khodachenko et al. 2007a). In view of the fact that multiple close-in giant exoplanets, comparable in mass and size with the solar system Jupiter, exist and that it is unlikely that all of them began their life as 10 times or even more massive objects, one may conclude that additional factors and processes have to be taken into consideration in order to explain the protection of close-in exoplanets against of destructive non-thermal mass loss. In the following sections, we introduce a more complete model of magnetosphere of a giant gas exoplanet, which due to its consequent account of the specifics of close-in "hot Jupiters" provides under similar conditions larger sizes for the planetary magnetospheric obstacles than those given by the simple screened magnetic dipole model, addressed in this section and considered so far in the literature.

4. THERMAL MASS LOSS OF CLOSE-IN HYDROGEN-RICH GAS GIANTS

As shown by Yelle (2004, 2006), Tian et al. (2005), García Muñoz (2007), Penz et al. (2008), Lammer et al. (2009), and Koskinen et al. (2010) the majority of the stellar X-ray and EUV radiation ($\lambda < 1000$ Å) is absorbed in the thermospheres of hot gas giants where it heats, ionizes, and dissociates a large fraction of the upper atmospheric neutral gas, turning it to the hydrodynamic expansion and outflow. By this, thermal atmospheric hydrogen loss of "hot Jupiters" is known to be caused mainly by the EUV radiation which is absorbed at higher atmospheric altitudes, populated mostly by atomic and ionized hydrogen. X-ray radiation is absorbed in lower atmospheric layers dominated by molecules.

Observations of solar proxies of different age, performed with the *ASCA*, *ROSAT*, *Extreme-Ultraviolet Explorer*, *Far-Ultraviolet Spectroscopic Explorer,* and *IUE* satellites, cover a range from 1 Å to 3300 Å, except for a gap in the EUV between 360 Å and 920 Å. This gap corresponds to a region of very strong interstellar medium absorption (Preibisch & Feigelson 2005) and requires a certain flux calibration procedure as provided in Guinan & Ribas (2002) and Ribas et al. (2005). It is a common practice to use the spectral range of 1–200 Å as a proxy for the adjacent EUV part of the electromagnetic spectrum (Lammer et al. 2009; Leitzinger et al. 2011). Full spectral irradiance (X-ray and EUV, i.e. XUV) tables, completed for a sample of solar proxies within the Sun in Time project (*EK Dra* [130 Myr], π^1 *UMa* [300 Myr], κ^1 *Cet* [750 Myr], β *Com* [1.6 Gyr], and β *Hyi* [6.7 Gyr]), show an excellent correlation between the emitted flux and stellar age (Ribas et al. 2005). In the course of this study, Ribas et al. (2005) deduced a scaling law for the XUV luminosity evolution of a Sun-like G-type star in the wavelength range 1–1700 Å. Here we use this scaling law for the determination of stellar XUV flux in order to estimate the thermal mass loss of a "hot Jupiter," orbiting a 4 Gyr old solar-analog G-type star.

Hydrodynamic escape of atmospheric gas and the related planetary thermal mass loss $dM_p^{(th)}/dt$ was modeled numerically in Yelle (2004, 2006), Tian et al. (2005), García Muñoz (2007), and Penz et al. (2008). At the same time, it has been shown recently that the results of these sophisticated models can be reproduced using a modified energy-limited approximation with inclusion of a certain radiative heating efficiency η, as well as tidal heating and Roche lobe effects (Erkaev et al. 2007; Penz et al. 2008; Lammer et al. 2009; Leitzinger et al. 2011):

$$\frac{dM_p^{(th)}}{dt} = \frac{3\eta F_{XUV}}{4G\rho_p(t)K(\xi)}, \quad (3)$$

where F_{XUV} is the stellar XUV flux at the orbital distance of a planet, G is gravitational constant, $\rho_p(t)$ is the mean planetary density, and $K(\xi) = 1 - 3/2\xi + 1/2\xi^3$ is a function of Roche lobe radius $\xi = r_{R.l.}/r_p$ measured in planetary radii (Erkaev et al. 2007). The heating efficiency η in Equation (3) is defined as the ratio of the net heating rate to the rate of stellar energy absorption. Recent studies have shown that realistic values of this parameter lie between 15% and 30% (Lammer et al. 2009; Chassefière 1996; Murray-Clay et al. 2009).

Figure 3 shows the dependence of the thermal mass-loss rate for a Jupiter-type test planet orbiting a solar-analog star

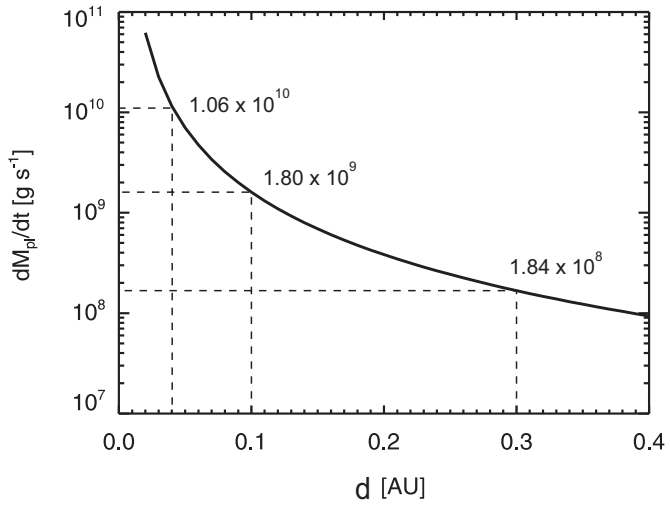


Figure 3. Thermal mass-loss rate for a Jupiter-type test planet orbiting a solar-analog star as a function of orbital distance of the planet, calculated with Equation (3).

as a function of orbital distance of a planet calculated with Equation (3). A heating efficiency $\eta = 30\%$ and the XUV flux for a 4 Gyr old G-type star (Ribas et al. 2005) were used in these calculations.

Three particular cases of the mass-loss rates for a Jupiter-type test planet at three different orbital distances d around a solar-analog star, followed from the model described by Equation (3), are summarized in Table 3 for further study. The last column in Table 3 provides the corresponding values of an XUV flux at different orbits around the star. As can be seen from Figure 3 and Table 3 the mass-loss rates of a hypothetical Jupiter analog exoplanet may reach significant values, up to $\sim 10^{10}$ g s^{-1}, if the planet orbits close to its host star ($\sim$0.045 AU). Such a large escape of planetary atmospheric material, ionized then by the stellar radiation, appears as a source of plasma and a driver for the formation of extended magnetodisks.

5. PARABOLOID MODEL OF A "HOT JUPITER" MAGNETOSPHERE

The paraboloid model approach to the study of planetary magnetospheres has been elaborated in detail during the last decades in a variety of papers devoted to the solar system planets (see Alexeev et al. 2003; Alexeev & Belenkaya 2005; Alexeev et al. 2010 and references therein). Originally the PMM was proposed for the study of the terrestrial magnetosphere (Alexeev 1978; Alexeev & Bobrovnikov 1997; Alexeev et al. 2003), but later it has been generalized and widely applied for the modeling of the magnetospheres of Jupiter and Saturn (Alexeev & Belenkaya 2005; Alexeev et al. 2006; Belenkaya 2004, 2007, 2009; Belenkaya et al. 2005, 2006, 2007, 2008), as well as Mercury (Alexeev et al. 2008, 2010). These generalized models have been successfully tested against the magnetic field measurements performed by various spacecraft (Mercury: *Messenger*; Jupiter: *Ulysses* and Saturn: *Pioneer 11*, *Cassini*), showing good agreement between the PMM predictions and the in situ measured values. Therefore, the goal of the paper is not connected with justification of the PMM methodology. It consists in the application of the model to the case of a close-orbit giant exoplanet, in order to reveal a more realistic configuration of the magnetic field around such a planet and to estimate the size of the planetary magnetic obstacle. The typical

Table 3
Mass-loss Rates for a Jupiter-type ($M_p = M_J$, $r_p = R_J$, $\rho = 1.33$ g cm^{-3}) Test Planet Orbiting a Solar-analog G-type Star ($M_* = M_{Sun}$, $R_* = R_{Sun}$, Age 4 Gyr) at Different Orbital Distances d

d (AU)	P (day)	$dM_p^{(th)}/dt$ (g s^{-1})	F_{XUV} (erg cm^{-2} s^{-1})
0.045	3.49	1.06×10^{10}	2665.62
0.1	11.55	1.80×10^{9}	539.79
0.3	60.02	1.84×10^{8}	59.98

Note. The calculations are made with Equation (3), adopting a heating efficiency $\eta = 30\%$ and the XUV flux for a 4 Gyr old G-type star from Ribas et al. (2005).

characteristics of "hot Jupiters" and their surrounding stellar wind plasma environment summarized in the previous sections will be used as an input for the quantitative characterization of the magnetosphere of an exoplanet on the basis of the PMM. Below, we will repeat only some basic points of the PMM concept and after that will demonstrate the importance of magnetodisks in the scaling of magnetospheres of "hot Jupiters." This study sheds more light on the problem of "hot Jupiter"—stellar wind interaction and magnetospheric protection of planetary atmospheres against stellar wind erosion.

5.1. PMM—General Issues

The name of the model follows from its key simplifying assumption that the planetary magnetopause may be represented as a paraboloid of revolution, elongated in the direction of the stellar wind flow. The PMM calculates the magnetic field generated by a variety of current systems located on the boundaries and within the boundaries of a planetary magnetosphere. The main contributors to the magnetic field in PMM, in the most general case, are: (1) the planetary intrinsic magnetic dipole field; (2) the magnetic field of a current disk (magnetodisk) around the planet; (3) the magnetopause current, which provides confinement of the dipole and magnetodisk fields inside the magnetopause; (4) the cross-tail currents and their closure currents on the magnetopause; (5) the IMF, which partially penetrates into the magnetosphere as a result of reconnection with its magnetic field. The overall magnetic field produced by the magnetopause currents, magnetotail, and magnetodisk current systems is calculated using a method developed by Alexeev (1978). It ensures that the magnetic fields of various magnetospheric sources are confined within the area delimited by the paraboloidal shape magnetopause. This is achieved by the implementation of the appropriate shielding potential at the magnetopause border.

The PMM is formulated in the planetary-dipole-centered stellar-magnetospheric coordinate system (PSM), with the planetary magnetic dipole moment $\vec{\mathcal{M}}$ located in the xz-plane and the x-axis pointed toward the star. In the most general case, the following parameters characterize the structure of the planetary magnetosphere in the PMM shown in Figure 4 (Alexeev & Bobrovnikov 1997; Alexeev et al. 2003; Belenkaya et al. 2005; Alexeev & Belenkaya 2005): (1) the distance $R_1 \equiv R_s$ from the center of planet to the substellar point on the magnetopause; (2) the distance R_2 from the center of planet to the inner edge of the magnetospheric tail current sheet; (3) the outer and inner edges of the magnetodisk relative to the center of planet, e.g., R_{D1} and R_{D2}, respectively; (4) the value of the planetary dipole magnetic field $B_{d0} = B_d(r = r_p, z = 0)$ in the equatorial plane at the surface of planet; (5) the value of magnetic field $B_{DC} = B_{MD}(r = R_{D1}, z = 0_{\pm})$ produced by the magnetodisk

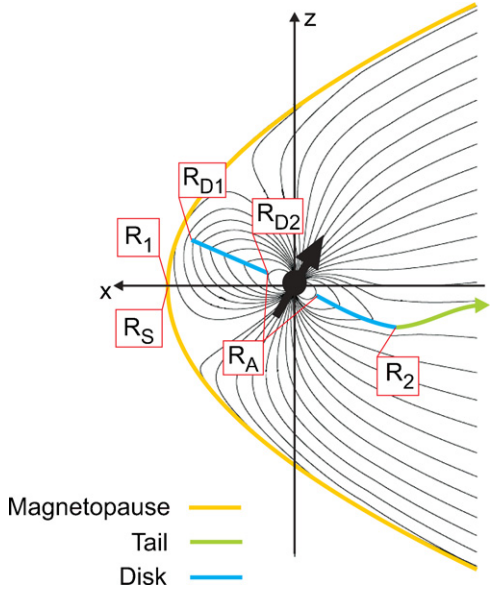


Figure 4. Schematic view of the major scales and current sources in the PMM.

at its outer edge; (6) the value of magnetic field B_t/α_0 produced by the current sheet alone at the inner edge of the magnetotail current sheet (e.g., for $r = R_2$), where $\alpha_0 = (1 + 2R_2/R_1)^{1/2}$; (7) the magnetic dipole tilt angle ψ relative to the z-axis; (8) the displacement z_0 of the magnetotail current sheet relative to the magnetic equatorial plane $z = 0$; and (9) the portion, **b**, of the IMF, **B**, penetrating into magnetosphere, given as $\mathbf{b} = k_r\mathbf{B}$, where k_r is the reconnection efficiency coefficient (Slavin & Holzer 1979).

The shape of the magnetopause in the PMM is approximated by a paraboloid of revolution defined as follows:

$$2xR_1 = 2R_1^2 - y^2 - z^2. \quad (4)$$

The appropriateness of such a shape for the forward magnetopause is supported by the boundary fit of Russell (1977) and Slavin et al. (2009). In particular, based on Mariner 10 observations, Russell (1977) found that a near-paraboloidal shape of the real planetary magnetopause is characterized by an eccentricity of 0.8 whereas a true parabola has an eccentricity of 1.0.

In the present paper we consider a simplified version of the PMM, assuming an orthogonal orientation of the planetary magnetic dipole relative to the stellar wind plasma flow (e.g., $\psi = 0$), no displacement of magnetotail current sheet (e.g., $z_0 = 0$), and without taking into account the IMF. Additional details regarding the major elements of PMM and their mathematical representation including the key equations are given in the Appendix for the sake of completeness.

5.2. Magnetodisk—a Key Element of a "Hot Jupiter" Magnetosphere

According to the model, a magnetodisk is placed in the equatorial plane at the interval of radial distances $[R_{D2}, R_{D1}]$ from the center (see Figure 4). The formation of a magnetodisk is schematically shown in Figure 5. It may be justified in the following way. It is well known that the field of a rotating planetary magnetic dipole can drive the inner magnetospheric plasma to rigid corotation with a planet only inside of the so-called Alfvénic surface, where the strength of the magnetic field is high enough (Mestel 1968; Vasyliunas 1983). The equatorial

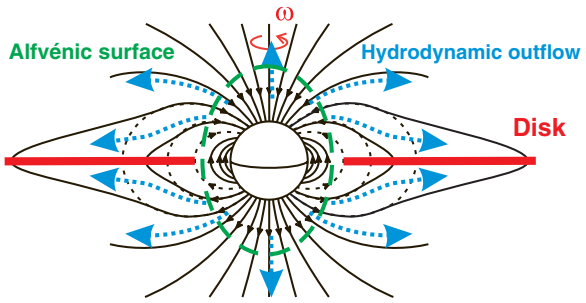


Figure 5. Schematic view of magnetodisk formation. The outflowing plasma, moving along the field lines inside the "Alfvénic surface" ($r < R_A$), is concentrated near the equatorial plane and provides the material source for the creation of a magnetodisk. The plasma, escaping along the filed lines, penetrating beyond the "Alfvénic surface," deforms the original planetary magnetic dipole field, resulting in the radial stretching of the field lines and the creation of a disk-type current sheet in the equatorial region.

boundary of the "Alfvénic surface," R_A, is determined from the equality of energy densities of the plasma rotational motion $\varepsilon_p = \rho_A\omega_p^2R_A^2/2$ and the dipole magnetic field $\varepsilon_B = M_d^2/2\mu_0R_A^6$, where $M_d = \mu_0\mathcal{M}/(4\pi)$ (Mestel 1968; Coroniti & Kennel 1977).

Beyond the "Alfvénic surface" ($r > R_A$), i.e., in the area where the rotating planetary dipole magnetic field becomes too weak to drive the plasma in rigid corotation, an outflow of the subcorotating material begins. The fact of rigid corotation within the "Alfvénic surface" assumes a strong coupling between the rotating magnetic field and the magnetospheric plasma, which in turn requires sufficiently high ionospheric electric conductivities. That is assumed to be the case in the present study. In the general case, a self-consistent treatment of the electric circuit, formed by the magnetospheric field-aligned currents caused by the loss of the rigid corotation of plasma and their closure in the planetary ionosphere, is needed (see, for example, Cowley et al. 2005). In the idealized case considered in the present paper, the material is supposed to be in a free flow regime at $r > R_A$, i.e., the total sum of forces acting on an elementary volume of plasma is zero, and its velocity V_{esc} remains constant. The material, released in the free flow at the Alfvénic radius distance with the local corotation angular velocity $V_{cor}(r = R_A) = \omega_pR_A$, will keep this motion further, and at some distance $r > R_A$, the local escaping velocity will have a radial and an azimuthal component. By this, the radial component, given as $V_{esc}^{(r)}(r) = V_{cor}(r = R_A)(1 - (R_A/r)^2)^{1/2}$, at large distances (e.g., for $r \gg R_A$) will be $V_{esc}^{(r)} \sim V_{cor}(r = R_A) = \omega_pR_A$. Therefore, the inner edge of the disk may be taken as approximately coinciding with the "Alfvénic surface" radius, i.e., $R_{D2} \approx R_A$. Such a centrifugal inertial mechanism for plasma outflow may be compared with the similar escape of a stone from a sling. On the other hand, even without the "sling-type" acceleration, the hydrodynamically escaping partially ionized upper atmospheric material due to thermal mass loss (e.g., "thermal wind") contributes an additional outflow component which is not distinguished at the present moment from the centrifugal inertial part in the total expanding plasma flux V_{esc}. Altogether, a detailed study of the magnetodisk formation and the relative role of the "sling-type" and "thermal wind" mechanisms is an actual task, which has to be performed with the help of numerical simulations, in order to make possible quantitative magnetosphere studies for particular exoplanets. It stays, however, beyond the scope of the present paper, which deals only with one aspect of this complex problem—how

the presence of a magnetodisk may change the size of an exoplanetary magnetosphere.

One of the first cases when a magnetodisk model similar to that has been discussed is the paper by Mestel (1968). The author considers there the escape of plasma from a rotating magnetized star and proposes distinguishing two zones in the stellar wind flow: first, a "dead zone" where the roughly dipolar field of a star is strong enough to force the plasma flow to follow the field and to keep the gas co-rotating with a star, and second, a "wind zone" where the gas flow drags the field to follow the flow, resulting in the formation of an open-field lines region. By this, the "Alfvénic surface," which crosses the equatorial plane at $r = R_A$, separates these two zones (see Figure 5). Already in this work, two possibilities for the creation of an outflowing material flux were addressed. One is related to the pressure gradient-driven "thermal wind," caused by the high temperature of the expanding stellar corona, and another due to the magnetically controlled centrifugal forces which drive a "centrifugal wind." The last becomes important if the coronal temperature is too low for driving a thermal wind. In that sense the situation is similar to the "hot Jupiter" case considered here, when the thermal expansion of the heated and ionized planetary upper atmosphere takes place under the conditions of a rotating planetary intrinsic magnetic dipole field.

The outflowing plasma, moving along the field lines inside the "Alfvénic surface" ($r < R_A$), is concentrated near the equatorial plane and provides the material source for the creation of the magnetodisk. The plasma, escaping along the field lines and penetrating beyond the "Alfvénic surface," deforms the original planetary magnetic dipole field and results in the radial stretching of the field lines (Mestel 1968) and the creation of a disk-type current sheet (of at least several Larmor radii thickness) in the equatorial region. At the same time, thermal atmospheric escape itself may appear not only as a source of plasma for the disk, which compensates for the material loss (e.g., centrifugal inertial expansion and non-thermal mass loss) at the magnetosphere boundary, but also appears as an additional driver for shaping the disk and the whole magnetosphere. The situation with the magnetodisk formation and confinement beyond R_A is characterized by continuous load of plasma to the disk, as well as to the entire magnetosphere, and simultaneous loss of the expanding material from the system by the non-thermal mechanisms at the boundary of the magnetosphere.

Therefore, the specifics and essential difference of the considered exoplanetary magnetodisks, compared to the magnetodisks of solar system planets (Caudal 1986; Achilleos et al. 2010), assumes the presence of material sources and sinks, which provide continuous flow of the material through the system. Analytic solutions for a kinematic model of a stationary electromagnetic field and electric current environment around a rotating magnetized sphere (with a dipole-type magnetic field) in the presence of an axisymmetric radial outflow of plasma have been considered in Alekseev et al. (1982). Magnetic field configuration obtained there clearly indicates the formation of a thin equatorial current disk.

The ring electric current of the disk is determined by the magnetic flux above (and below) the disk (Alexeev & Belenkaya 2005). This flux is a part of the total magnetic flux of the planetary dipole which corresponds to the dipolar field lines extended outside the "Alfvénic surface," i.e., the lines which in the case of an undisturbed magnetic dipole would cross the equatorial plane beyond the "Alfvénic surface" radius R_A. Contrary to the dipole field case, these lines are elongated almost parallel to the equatorial plane and have, in the case of a highly conducting plasma, a component $B_\theta \sim 0$. In the considered disk model the magnetic flux above (and below) the disk is assumed to be conserved, i.e., independent of the distance. This is true for a very high ($\rightarrow \infty$) conductivity of the disk plasma. Under this condition the pressure of the magnetic field outside the disk may be considered to be the same as the pressure of plasma at the disk center. Further details on the disk current and magnetodisk field can be found in the Appendix.

The density of plasma at the inner edge of the disk ρ_A may be estimated from the planetary thermal mass loss $dM_p^{(th)}/dt$, considered in Section 4. Let us assume that the portion $\gamma(dM_p^{(th)})/dt$ of the total thermally escaping material takes part in the formation of the magnetodisk. In this case $\gamma(dM_p^{(th)})/dt = 2\pi R_A^2 \delta\theta \rho_A V_{esc}$, where $\delta\theta$ is the angular thickness of the disk. Using this expression one can write

$$\rho_A = \frac{\gamma(dM_p^{(th)}/dt)}{2\pi R_A^2 \delta\theta V_{esc}} \quad . \tag{5}$$

From the equality of the above-defined energy densities of the plasma rotational motion ε_p and the dipole magnetic field ε_B, using Equation (5) we obtain the expression for the equatorial radius of the "Alfvénic surface," or the inner radius of the disk R_{D2}, measured in the planetary radii r_p:

$$\frac{R_A}{r_p} = \frac{R_{D2}}{r_p} = \left(\frac{2\pi \delta\theta B_{d0}^2 V_{esc}}{\mu_0 \omega_p^2 \gamma(dM_p^{(th)}/dt)} \right)^{1/6} , \tag{6}$$

where $B_{d0} = B_d(r = r_p, z = 0)$ is the value of the planetary dipole magnetic field at the surface of the planet in the equatorial plane. When obtaining Equation (6) we took into account that $M_d = B_{d0} r_p^3$.

Now let us specify a value of the factor γ in Equations (5) and (6). First of all, the escaping upper atmospheric material is only partially ionized, and the neutral fraction has to be excluded from the consideration of the plasma magnetodisk build-up. According to the recent aeronomical calculations of the upper atmospheric structure of giant exoplanets at close orbits (Yelle 2004; García Muñoz 2007; Koskinen et al. 2010) with inclusion of the major photochemistry processes of atmospheric species, the expanding material at the heights above $3r_p$ is mostly ionized with the ratio of ion to neutral number densities of about 10 (Yelle 2004). Therefore, in order to take into account the contribution of only ionized part of the escaping mass, one has to use in the calculations a weight coefficient $10/11 \sim 0.9$ before the total thermal mass-loss rate $dM_p^{(th)}/dt$. At the same time, the coefficient γ has to reflect also the fact that not all the escaping and ionized material contributes to the creation of the magnetodisk. There is a part of plasma flow which is lost along the open field lines. Since motion of the escaping plasma happens mostly along the field lines, we may assume that the escaping material flux is proportional to the magnetic field flux. The total flux of the non-disturbed magnetic dipole field, which would cross the equatorial plane beyond the planetary radius r_p, is $F_0 \equiv \int_{r_p}^{\infty} B_z(r, z = 0) r dr d\varphi = \int_{r_p}^{\infty} 2\pi (B_{d0} r_p^3 / r^3) r dr = 2\pi B_{d0} r_p^2$. Then, the portion of the dipole flux beyond the Alfvénic radius defined in the similar way is $(r_p/R_A)F_0$. According to the PMM calculations, this flux is divided in equal parts between the magnetic flux through the magnetodisk and the flux of open field lines going to the external

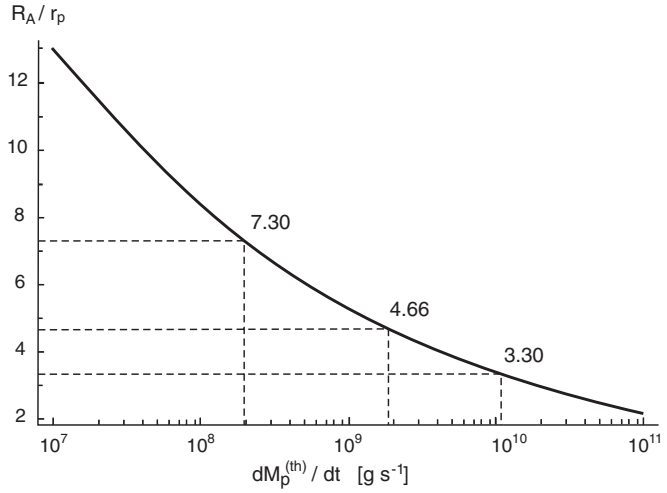


Figure 6. "Alfvénic surface" equatorial radius R_A of a "hot Jupiter" as a function of planetary thermal mass loss.

magnetosphere (Alexeev & Belenkaya 2005). Therefore, the part of plasma flow, lost along the open field lines, which does not take part in the formation of the magnetodisk, is the fraction $0.5(r_p/R_A)$ of the total escaping ionized material flow ($\sim 0.9(dM_p^{(th)})/dt$).

Finally, in view of the above given reasoning, taking into account the fact of partial ionization of the escaping material and its partial loss along the open field lines, the mass load to the magnetodisk may be estimated as approximately $0.9(1 - 0.5(r_p/R_A))$ of the total planetary atmospheric thermal mass loss. In other words, we have to take in Equations (5) and (6) the factor $\gamma = 0.9(1 - 0.5(r_p/R_A))$. This yields a more precise equation for the "Alfvénic surface" equatorial radius R_A:

$$\left(\frac{R_A}{r_p}\right)^5 = \frac{4\pi\delta\theta B_{d0}^2 V_{esc}}{\mu_0\omega_p^2 0.9(dM_p^{(th)}/dt)}\left(2\frac{R_A}{r_p} - 1\right)^{-1}. \quad (7)$$

Figure 6 displays the solution of Equation (7) as a function of the planetary thermal mass loss, assuming $V_{esc} \sim V_{cor} = \omega_p R_A$. This assumption corresponds to the case of a dominating centrifugal inertial material outflow outside the "Alfvénic surface," taken for the definiteness sake. This is an idealizing assumption, but in view of many other uncertainties regarding plasma and magnetic field parameters of "hot Jupiters," it may nevertheless be taken as a suitable simplification.

As can be seen in Figure 6, the values of R_A corresponding to the mass-loss rates typical for the Jupiter-type test planet at orbital distances between 0.045 AU and 0.3 AU fall in the interval from 3.3 r_p to 7.3 r_p and are high enough to neglect the dependence of factor γ on R_A in Equation (6). In other words, the plasma lost along the open filed lines does not affect strongly the overall value of mass load to the magnetodisk in the considered region of parameters. The effect of neutral fraction in the escaping material is also not too strong. Thus, without making a big mistake in estimation of R_A one may take $\gamma = 0.9(1 - 0.5(r_p/R_A)) \sim 0.9 \approx 1$ in Equation (6). This, keeping the assumption of $V_{esc} = \omega_p R_A$, will give the following expression:

$$\frac{R_A}{r_p} = \left(\frac{2\pi\delta\theta B_{d0}^2 r_p}{\mu_0\omega_p(dM_p^{(th)}/dt)}\right)^{1/5}, \quad (8)$$

which may be used for rough estimations of the R_A value in "hot Jupiters." The difference between the precise result followed from Equation (7) and the estimations given by Equation (8) does not exceed several percents of the last (e.g., (3–6)%). Such uncertainty does not produce any significant effect in the PMM calculations of a "hot Jupiter" magnetopause stand-off distance R_s.

In spite of the different physical mechanisms of the origin of the considered exoplanetary magnetodisks and the magnetodisks of Jupiter and Saturn in the solar system, the effect of their current systems on the large-scale magnetosphere structure, size, and topology, as it is treated by the PMM, remains similar. In that respect R_A of a "hot Jupiter" may be scaled also in the units of the "Alfvénic surface" radius R_{AJ} of the solar system Jupiter. Taking into account the proportionality of the planetary magnetic dipole moments to a certain power k of ω_p (see Equation (1)), we can write that $B_{d0}/B_{d0J} = \omega_p^k/\omega_J^k$, where B_{d0J} is the Jovian magnetic dipole field at the surface of the planet in the equatorial plane. Then, using the estimative equation (8) and assuming a similarity of the magnetodisk geometric parameters (e.g., $\delta\theta$) for the considered hypothetic "hot Jupiter" and the solar system Jupiter, we obtain

$$\frac{R_A}{R_{AJ}} = \left(\frac{\omega_p}{\omega_J}\right)^{(2k-1)/5}\left(\frac{dM_J/dt}{dM_p^{(th)}/dt}\right)^{1/5}. \quad (9)$$

Note that in the case of $k = 1/2$, i.e., with the planetary magnetic dipole scaling model of Stevenson (1983), the ratio R_A/R_{AJ}, according to Equation (9), is controlled only by the mass-loss rate and does not depend on the planetary angular velocity. This case is considered in further calculations of the particular parameters of "hot Jupiter" magnetospheres.

5.3. Magnetodisk-dominated Magnetosphere of a "Hot Jupiter"

The inclusion of the magnetodisk and magnetotail into consideration cardinally changes the estimation of the substellar magnetopause stand-off distance R_s, addressed in Section 3 and considered in more detail in Grießmeier et al. (2004, 2007a). The difference consists of the necessity to take into account in the substellar point pressure balance not only the magnetic field pressure of the screened planetary magnetic dipole field, but also the total pressure. The latter is comprised of the pressure of the total magnetic field, jointly produced by the screened magnetic dipole, magnetodisk, and magnetotail, as well as of the disk plasma pressure p_{mp}. The PMM provides a self-consistent approach to the calculation of a three-dimensional magnetic field structure in a planetary magnetosphere and determines R_s, based on the consequent evaluation of the total magnetic field in the substellar point which incorporates the contribution of all above-mentioned components (current systems) of the model (i.e., magnetodisk, magnetotail, and magnetopause currents). The view of magnetic field lines in the zx-plane ($\phi = 0$ plane) of a "hot Jupiter" magnetosphere for a Jupiter-type planet orbiting at different distances around a solar-analog star is shown in Figure 7.

The basic role of the magnetodisk in the scaling of the magnetosphere of a close orbit "hot Jupiter" may be illustrated using a simplified non-self-consistent (additive) approach which we outline briefly below. On the one hand, this simplified estimation enables us to see a basic trend; on the other hand, it is used as a first-order approximation for obtaining the initial

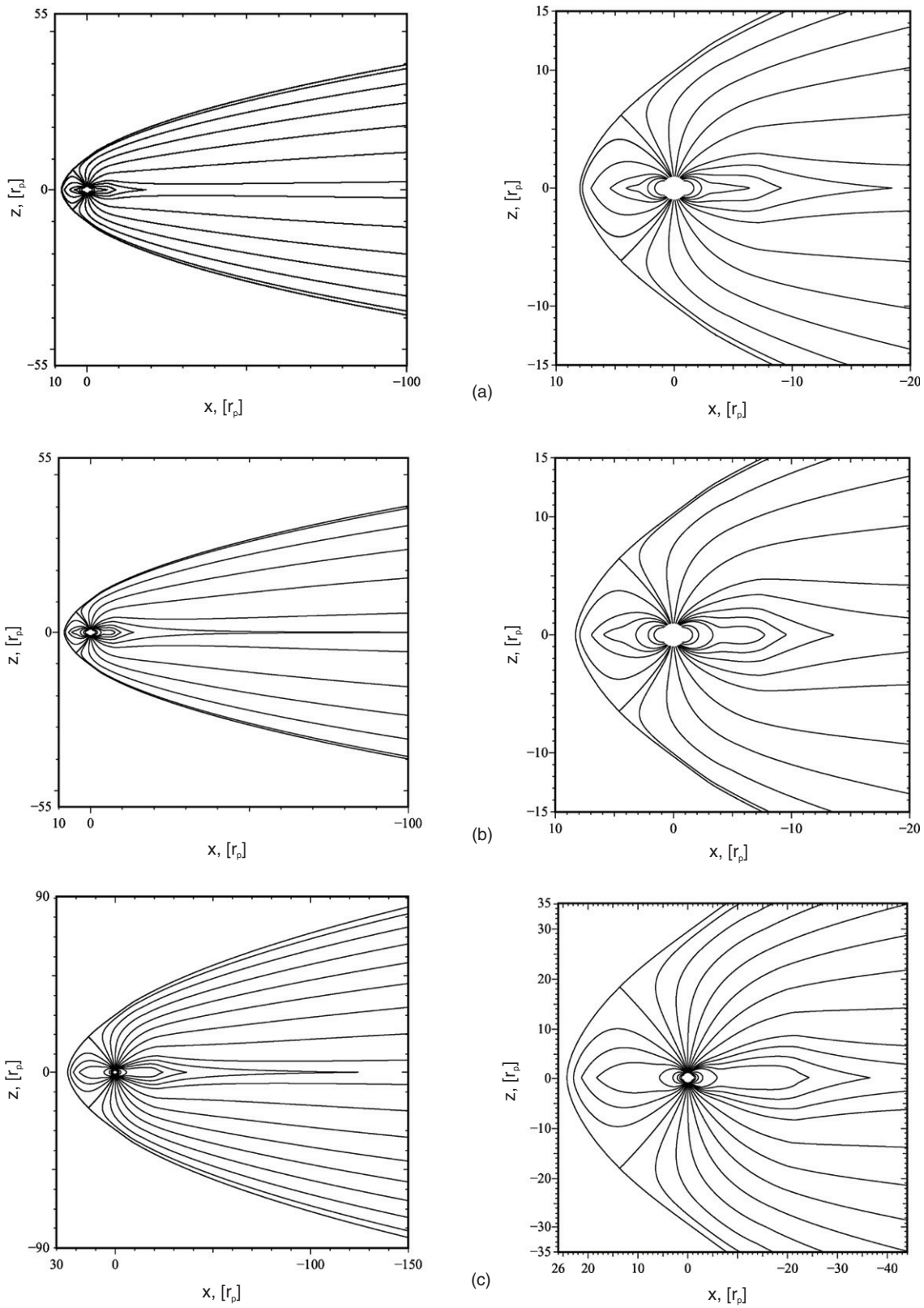


Figure 7. Magnetic field lines (left panel shows a zoomed view) in the *ZX*-plane ($\phi = 0$ plane) of a "hot Jupiter" magnetosphere for the Jupiter-type planet ($M_p = M_J$; $r_p = R_J$), orbiting at different distances around a solar-analog G-type star. (a) 0.045 AU, (b) 0.1 AU, and (c) 0.3 AU.

parameters of the magnetosphere, which are then adjusted to the self-consistent values via a chain of modeling iterations. This is a well-elaborated procedure inside the PMM, which has been successfully applied in the previous studies of Mercury, Earth, Jupiter, and Saturn (Alexeev et al. 2008, 2010, 2003; Alexeev & Belenkaya 2005; Alexeev et al. 2006; Belenkaya 2004, 2007, 2009; Belenkaya et al. 2005, 2006, 2007, 2008). According to the PMM view, a current-carrying plasma disk

is located beyond the "Alfvénic surface" radius, i.e., at $r > R_A$. Therefore, depending on the distance from the planet, we have a different character of the magnetic field decrease near the equatorial plane ($\theta = \pi/2$, or $z = 0$). Within the "Alfvénic surface" the field behaves as a dipole one, i.e., $\mathbf{B}(r, z = 0) = B_\theta(r)\,\theta_0 = B_{d0} r_p^3/r^3\,\theta_0$. Outside of the "Alfvénic surface" the character of the field is defined by the current disk, which according to Equations (A7) and (A9) results in $\mathbf{B}(r, z \sim 0) = B_r(r)\,\mathbf{r}_0 = B_{d0} r_p^3/(R_A r^2)\,\mathbf{r}_0$, where the relation $B_{DC} R_{D1}^2 = B_{d0} r_p^3/R_A$ has to be satisfied in order to keep continuity of the field at the boundary of the "Alfvénic surface" and to fulfill Equations (A9) at the same time. The pressure balance equation at the equatorial substellar point ($r = R_s$) in this case may be written as

$$p_{sw} \equiv \rho_{sw} \tilde{v}_{sw}^2 = \frac{\kappa^2 (B_{ds} + B_{MDs})^2}{2\mu_0} + p_{mp}\ , \qquad (10)$$

where p_{sw} denotes the dynamic pressure of stellar wind; $B_{ds} = B_\theta(r = R_s) = B_{d0} r_p^3/R_s^3$ and $B_{MDs} = B_{d0} r_p^3/(R_A R_s^2)$ are the values of the magnetic field produced at the substellar point by the dipole and magnetodisk, respectively. By this, we assume that the value of the magnetodisk field in the vicinity of R_s is about the value of $B_r(r = R_s)$ (see also in Figure 7). The coefficient $\kappa \approx 2.44$ is an amplifying factor of the inner magnetospheric field at the magnetopause (Alexeev & Bobrovnikov 1997; Alexeev et al. 2003), which is required to take into account the contribution of the Chapman–Ferraro field at the substellar point. It is connected with the form factor f_0 from Equation (2) as $\kappa = 2 f_0$. The pressure of the magnetodisk plasma at the substellar point may be estimated from the requirement of balance between the magnetic field pressure in the close vicinity of the disk and plasma pressure inside the disk: $p_{mp} = (B_{d0}^2 r_p^6/R_A^2 R_s^4)(1/2\mu_0)$, which ensures the confinement of the highly conductive disk. Taking into account all these factors, one may obtain from Equation (10) an equation for R_s/R_A:

$$\kappa^2 + 2\kappa^2 \frac{R_s}{R_A} + (1 + \kappa^2)\frac{R_s^2}{R_A^2} - \frac{2\mu_0 p_{sw} R_A^6}{B_{d0}^2 r_p^6}\frac{R_s^6}{R_A^6} = 0\ . \qquad (11)$$

This polynomial equation relative to R_s/R_A can be solved numerically. That will give a rough non-self-consistent estimate for the magnetosphere size at the substellar point $R_s \equiv \tilde{R}_s^{(dip+MD)}$, caused jointly by the planetary dipole and magnetodisk. Note that the account of the effects of plasma pressure in the total pressure balance results in the appearance of a unit in brackets in the third term in Equation (11). As it follows from Equations (10) and (11), the contribution of plasma pressure is $\kappa^2 = 5.95$ times less than the contribution of the magnetic field pressure of the magnetodisk and the corresponding magnetopause currents.

To understand the general trend in variation of R_s as a function of the planetary mass-loss rate and angular rotation speed ω_p one may consider a reduced equation $(1 + \kappa^2)(R_s^2/R_A^2) - (2\mu_0 p_{sw} R_A^6/B_{d0}^2 r_p^6)(R_s^6/R_A^6) = 0$ which follows from Equation (11) after neglecting the low-power terms for sufficiently large R_s/R_A. The analytic solution of this equation yields an approximate expression for R_s:

$$\frac{R_s}{r_p} \equiv \frac{\tilde{R}_s^{(dip+MD)}}{r_p} \sim \frac{B_{d0}^{1/2}(1 + \kappa^2)^{1/4}}{(2\mu_0 p_{sw})^{1/4}} \left(\frac{R_A}{r_p}\right)^{-1/2}\ . \qquad (12)$$

Taking into account Equation (9) and the proportionality of the planetary magnetic dipole moments to certain power k of ω_p (see Equation (1)), Equation (12) may be rewritten in terms of the known Jovian values (R_{AJ}, dM_J/dt, and B_{d0J}):

$$\frac{R_s}{r_p} \equiv \frac{\tilde{R}_s^{(dip+MD)}}{r_p} \sim \frac{B_{d0J}^{1/2}(1 + \kappa^2)^{1/4}}{(2\mu_0 p_{sw})^{1/4}} \left(\frac{R_{AJ}}{r_p}\right)^{-1/2} \times \left(\frac{\omega_p}{\omega_J}\right)^{(3k+1)/10} \left(\frac{dM_p^{(th)}/dt}{dM_J/dt}\right)^{1/10}\ . \qquad (13)$$

Therefore, according to Equation (13), for a given p_{sw} the size of the magnetosphere should increase for the increasing planetary angular velocity ω_p and/or thermal mass-loss rate $dM_p^{(th)}/dt$.

Table 4
"Hot Jupiter" Magnetopause Stand-off Distance at Substellar Point R_s and Its Major Control Parameters

d (AU)	$R_s^{(dip+MD+tail)}$ (r_p)	$\tilde{R}_s^{(dip+MD)}$ (r_p)	$R_s^{(dip)}$ (r_p)	R_A (r_p)	$\mathcal{M}_{MD}/\mathcal{M}$	ω_p (ω_J)	$dM_p^{(th)}/dt$ (g s^{-1})
0.045[a]	8.0	9.27	5.76	3.30	1.64	0.118	1.06×10^{10}
0.1[a]	8.27	9.06	6.16	4.66	1.29	0.036	1.80×10^{9}
0.3[b]	24.2	25.6	15.0	7.30	3.59	1.0	1.84×10^{8}
5.2[c]	71.9	69.3	41.8	19.8	3.32	1.0	1.0×10^{6}

Notes. $R_s^{(dip+MD+tail)}$ is given by PMM taking into account screened planetary dipole, screened magnetodisk, and magnetotail currents; $\tilde{R}_s^{(dip+MD)}$ is a non-self-consistent estimation of R_s followed from Equation (11); $R_s^{(dip)}$ is an estimation of R_s for the case of only a dipole-type magnetosphere given by Equation (2) with the magnetic dipole moment provided by the model from Stevenson (1983).
[a] Tidally locked.
[b] Not tidally locked.
[c] Jupiter.

Table 4 provides a summary of the PMM-simulated values of the magnetopause stand-off distance $R_s = R_s^{(dip+MD+tail)}$ at the substellar point for different orbital locations of a hypothetical exoplanet near its host star and compares these values to those provided by the non-self-consistent estimations of R_s given by Equation (11) (e.g., $\tilde{R}_s^{(dip+MD)}$) and the values corresponding to the case of only a dipole-type magnetosphere $R_s^{(dip)}$ (i.e., without the magnetodisk) given by Equation (2). A Jupiter-type exoplanet and a solar-analog star are taken for these calculations. By this, for the estimation of the planetary magnetic dipole moment for the gravitationally locked orbits (e.g., 0.045 AU and 0.1 AU) a model with $\mathcal{M} \propto \omega_p^{1/2}$ has been taken (Stevenson 1983). In the bottom line of Table 4 we provide for comparison the corresponding parameters of the solar system Jupiter. Note that the magnetodisk mass load in the case of the solar system Jupiter, caused mainly by its satellite Io's volcanic activity, is two to four orders of magnitude less than that for the "hot Jupiter," resulting in the thermal mass-loss of the planetary atmosphere.

Due to the screening of the inner magnetospheric sources by magnetopause currents, their contribution to the real magnetic field value will be different from that used in course of the non-self-consistent estimations in Equations (10) and (11). This causes the difference between the values $R_s \equiv R_s^{(dip+MD+tail)}$ obtained with the PMM and the non-self-consistent estimates, followed from Equation (11).

As can be seen in Table 4, the magnetodisk, whose parameters change with the orbital distance of a planet, increases considerably (up to 40%–70%) the size of the magnetosphere, compared to a simple dipole-type magnetosphere. The contribution of the magnetodisk to the total field in the substellar point and therefore in the pressure balance, which defines

R_s, in all cases is higher than that of the planetary magnetic dipole. The ratio of magnetodisk and planetary dipole magnetic moments $\mathcal{M}_{MD}/\mathcal{M}$ is always >1. This gives a reason to speak about a *magnetodisk-dominated magnetosphere* of a "hot Jupiter." Such more extended magnetospheres of "hot Jupiters" may be efficient protectors for the upper atmospheres of close-in planets against extreme stellar wind erosion.

6. DISCUSSION AND CONCLUSIONS

Based on the PMM concept, we introduce in the present paper a more complete view of an exoplanetary magnetosphere compared to that assumed in previous studies. It has been applied to the case of a close orbit "hot Jupiter" with a continuously expanding and outflowing hydrogen-rich upper atmosphere. The advantage of the PMM consists in the consequent account of a whole variety of magnetospheric key current systems and magnetic field sources. Of special importance, in the context of exoplanetary physics, is the flexibility of the PMM with respect to the modeled object, and a possibility to apply it to the reconstruction of magnetospheres of different types of exoplanets. The PMM was successfully applied in the magnetosphere study of solar system planets and resulted in good agreement with the spacecraft in situ measurements. However, it is in the present work where the model is applied to exoplanets for the first time.

The key element and major specifics of the "hot Jupiter" magnetosphere considered in this work consist of the presence of a magnetodisk. The expanding and escaping upper atmospheric gas, heated and ionized by the stellar radiation, contributes to the build-up of the magnetodisk around the planet. The rotation (even slow) of the planetary magnetic dipole plays an important role in this process too. The magnetodisk is assumed to be located outside the "Alfvénic surface," at which the equality of energy of the planetary dipole magnetic field and of the co-rotating plasma kinetic energy is achieved. Beyond this surface the rotating magnetic field of a planet cannot drive equatorial plasma in rigid corotation, and the outflowing plasma changes the topology of the magnetic field by creating an equatorial current sheet of the disk. Taking the thermal mass loss of a "hot Jupiter" as the material source for the equatorial plasma disk requires that the particle escape height be less than the inner radius of the disk, i.e., R_A. Such an assumption seems to be a realistic one in view of the recent estimates of the upper thermosphere structure for close-in "hot Jupiters" such as HD209458b (Koskinen et al. 2010), which yields the values of about three planetary radii. Above these heights the atmosphere of HD209458b is mostly ionized. According to the picture adopted in this paper, a "hot Jupiter's" thermal mass-loss process should also play an important role (as the major material source) in the build-up of a magnetodisk and in shaping the planetary magnetosphere. Ions picked up by the stellar wind (e.g., Khodachenko et al. 2007a), as well as production of hot atomic hydrogen (energetic neutral atoms (ENAs)) coronas (by charge exchange between the neutrals of the expanding planetary atmospheric material and the protons of the stellar wind (Holmström et al. 2008; Ekenbäck et al. 2010)), provide the major contribution to the mass loss of a close-in "hot Jupiter." These processes are nowadays under an extensive study with the inclusion of the whole complex physics (species interaction, ionization, and photochemistry). The information on a realistic size and shape of the exoplanetary magnetosphere, which our work intends to provide, is of significant importance for this study.

Stellar wind interaction with "hot Jupiters" has been simulated numerically, using resistive MHD, by Ip et al. (2004) (extremely close-in case, no shock) and by Preusse et al. (2007). The formation of induced magnetospheres near moderately close-in unmagnetized terrestrial-type exoplanets has been modeled by Lipatov et al. (2005) on the basis of a hybrid code and in the drift-kinetic approximation, as well as by Johansson et al. (2009), using a hybrid code. However, in all of these numerical studies the planetary obstacle has been implemented just as a spherical boundary at which zero particle velocity and constant density were imposed together with the prescribed particle removal and production mechanisms to model surface absorption and atmosphere expansion. Therefore the effects of rotating planetary intrinsic magnetic fields and corresponding electrodynamics of the surrounding plasma, including the formation of planetary magnetodisks, were not incorporated into these models.

The performed modeling clearly indicates that the presence of a magnetodisk distinctively changes the character of the magnetosphere of a close orbit giant exoplanet which appears to be a magnetodisk-dominated one, in contrast to the dipole-dominated magnetospheres traditionally assumed in the previous studies. The magnetodisk-dominated magnetospheres of close-orbit "hot Jupiters" with a strong mass loss appear to be a new type of planetary magnetospheres which have no analogues among the planets of the solar system. They require, therefore, a special further investigation.

A more realistic structure of a "hot Jupiter" magnetosphere predicted by the PMM and its up to 40%–70% larger size, compared to a simple dipole-type magnetosphere case, have important consequences for the study of the magnetospheric protection of close orbit exoplanets, as well as for the investigation of the formation of extended ENA coronas around exoplanets (Holmström et al. 2008; Ekenbäck et al. 2010; Lammer et al. 2011). In particular, based on the modeling of the ENA production around the "hot Jupiter" HD209458b and subsequent fitting of the planet's transit Lyman-α spectra, Ekenbäck et al. (2010) reported about the size of the magnetospheric obstacle of the planet that $R_s \approx (4\text{–}10) \times 10^8$ m $\approx(5.6\text{–}13.9)\, r_p \sim (4.2\text{–}10.5)\, R_{HD209458b}$. The estimations of R_s for this planet, assuming only a magnetic dipole-type magnetosphere (Khodachenko et al. 2007a), give rather small values for the magnetopause stand-off distance. This means that the planetary dipole alone cannot provide the size of the magnetosphere of HD209458b, which may fit the magnetospheric obstacle size estimations followed from the ENA measurements (Holmström et al. 2008; Ekenbäck et al. 2010; Lammer et al. 2011). At the same time, as has been shown in our study (Table 4), the inclusion of a magnetodisk can easily add several planetary radii to the R_s value. If in the future it will be possible to obtain an independent estimation for an exoplanet's R_s, e.g., using the measurements of ENA clouds around a planet (Holmström et al. 2008; Ekenbäck et al. 2010; Lammer et al. 2011), or by transit curve asymmetry analysis (Vidotto et al. 2011; Llama et al. 2011), or via the detection of the planetary radio emission (Grießmeier et al. 2007b; Zarka 2007), then the PMM predictions for R_s may be used to judge the realistic values of the planetary intrinsic magnetic dipole moment, corresponding magnetodisk, and parameters of the stellar wind. This will open a way to perform remote diagnostics of the whole stellar-planetary system.

We assumed in the present study that the host star for a "hot Jupiter" is a solar-analog G-type star. In this case, in order to be able to apply the standard version of the PMM which supposes a super-Alfvénic stellar wind flow encountered by an exoplanet, we have to ensure that the closest considered orbit (0.045 AU) of the considered hypothetical exoplanet is located outside of the stellar Alfvénic sphere, at which the equality of the stellar wind speed and the local Alfvén speed is achieved. This stellar Alfvénic sphere should not be mixed with the "Alfvénic surface" around a planet, addressed in the paper in the context of disk formation. Taking the stellar wind parameters from Table 1, one can obtain that this condition is satisfied at the closest considered planetary orbit (0.045 AU) if the stellar dipole magnetic field there is less than 1066 nT. This corresponds to the dipole magnetic field at the stellar equatorial surface and poles less than 9.65 G and 19.3 G, respectively. That is similar to the situation on the Sun. The capability of the PMM to take into account a wide range of environmental conditions and the IMF (quiet and disturbed) affected by stellar activity processes opens a broad perspective for further application of the model in the investigation of the dynamics of exoplanetary magnetospheres. The next step on this way would be a consequent inclusion of the effects of IMF, as well as the incorporation of the temporal variation of the stellar wind parameters (i.e., inclusion of CMEs, shocks, and streams). The preliminary modeling estimations in Belenkaya et al. (2010) show that the tail current system and the magnetodisk ring current, as well as the intrinsic magnetic dipole, play a significant role in the reconnection between the IMF and the exoplanetary magnetospheric magnetic fields. At the same time, the direction of the stellar coronal magnetic field just slightly modifies the substellar magnetopause distance R_s. It changes dramatically, however, the size of the region occupied by the field lines connected with the planet on the night side. Therefore, the IMF direction controls the overall exoplanetary magnetospheric topology and scale. But this is a subject for a separate study which is now in progress.

This work was supported by the Austrian Fond zur Förderung der wissenschaftlichen Forschung (projects P21197-N16, I199-N16, and P22950-N16). The authors are thankful to the European FP7 project IMPEx (No.262863) and the subdivisions of the European research infrastructure Europlanet-RI, the JRA3/EMDAF (European Modeling and Data Analysis Facility; http://europlanet-jra3.oeaw.ac.at) and Science Networking NA2 (working groups WG4 and WG5; https://europlanet-scinet.fi), for support of their scientific communication and collaboration exchange visits. M.L.K., H.L., I.I.A., and J.-M.G. acknowledge the support by the International Space Science Institute (ISSI, Bern, Switzerland) and the ISSI team "Characterizing sellar and exoplanetary environments." The work of I.I.A. and E.S.B. was partially supported by the Royal Society (London)/RFBR grant No. 09-02-92603-KO-a and RFBR grant No. 11-05-00894a. H.L. and M.L.K. acknowledge also the support by the Helmholz Alliance project "Planetary evolution and life."

APPENDIX

PMM: MAJOR BUILDING BLOCKS

Below, the major building blocks of the PMM applied for the modeling of a "hot Jupiter" magnetosphere are summarized.

A.1. Screened Magnetic Dipole

A solution of the problem of a screened planetary dipole field confined within a model magnetopause approximated by a paraboloid of revolution was for the first time obtained by Alexeev & Shabansky (1972). The authors presented a solution of the Laplace equation with a given potential derivative at the boundary (Neumann problem) by direct integration of the dipole magnetic field component normal to the magnetopause. The next step was made by Greene & Miller (1994), who provided the integral representations of the screened planetary dipole field within a paraboloidal magnetopause with an arbitrary magnetopause flaring angle (i.e., an arbitrary ratio of the dawn–dusk cross-section radius to the substellar stand-off distance R_s). An analogous approach has been applied in Belenkaya et al. (2005) for a detailed description of the screened planetary dipole field within a model magnetopause in the Jovian magnetosphere. The same method is used in this paper for the reconstruction of topology of an exoplanetary magnetosphere by means of the PMM.

The combined field created within the magnetosphere by the planetary magnetic dipole and the screening magnetopause current is defined by a scalar potential as $\mathbf{B}_{d+sd} = -\nabla U_{d+sd}$ with $U_{d+sd} = U_d + U_{sd}$, where U_d and U_{sd} are the corresponding scalar potentials which describe the dipole and the screening magnetopause current, respectively. In the case of planetary dipole, directed along the z-axis of the PSM coordinate system, the total scalar potential of the screened dipole magnetic field, confined within the area bounded by the paraboloidal magnetopause, is given by (Belenkaya et al. 2005)

$$U_{d+sd} = M_M \cos\varphi \int_0^\infty \lambda^2 J_1(\lambda) J_1(\lambda\alpha) \times \left(K_1(\lambda\beta) - I_1(\lambda\beta) \frac{K_1'(\lambda)}{I_1'(\lambda)} \right) d\lambda, \quad \text{(A1)}$$

where $J_1(\lambda)$ is the Bessel function of the first kind; $I_1(\lambda\beta)$ and $K_1(\lambda\beta)$ are the modified Bessel functions; and the coefficient $M_M = 2\mathcal{M}/R_1^2$ is determined by the planetary dipole moment $\mathcal{M}$ and the substellar magnetopause distance R_1. The primes in Equation (A1) indicate the derivatives with respect to the argument and (α, β, φ) are the parabolic coordinates associated with the dipole-centered PSM Cartesian coordinate system so that

$$\begin{aligned} x &= \frac{R_1}{2}(\beta^2 - \alpha^2 + 1)\ , \\ y &= R_1 \alpha\beta \sin\varphi\ , \\ z &= R_1 \alpha\beta \cos\varphi\ . \end{aligned} \quad \text{(A2)}$$

As can be seen from Equation (A1), the derivative of U_{d+sd} with respect to β turns to zero on the magnetopause surface $\beta = 1$, because $K_1'(\lambda) \equiv I_1'(\lambda)(K_1'(\lambda)/I_1'(\lambda))$. This means that the combined potential U_{d+sd}, defined by Equation (A1), confines the dipole magnetic field inside the paraboloidal shape magnetosphere. The components of this screened dipole magnetic field in the parabolic coordinates have the following form (Alexeev & Bobrovnikov 1997; Alexeev et al. 2003):

$$\begin{aligned} B_\alpha^{(d+sd)} &= -\frac{1}{R_1\sqrt{\alpha^2+\beta^2}} \frac{\partial U_{d+sd}}{\partial \alpha}\ , \\ B_\beta^{(d+sd)} &= -\frac{1}{R_1\sqrt{\alpha^2+\beta^2}} \frac{\partial U_{d+sd}}{\partial \beta}\ , \\ B_\varphi^{(d+sd)} &= -\frac{1}{R_1\alpha\beta} \frac{\partial U_{d+sd}}{\partial \varphi}\ . \end{aligned} \quad \text{(A3)}$$

A.2. Magnetotail Current System

The model of the magnetotail adopted for exoplanets is similar to that proposed previously for the terrestrial (Alexeev & Bobrovnikov 1997; Alexeev et al. 2003) and Jovian (Belenkaya et al. 2005) magnetospheres. The magnetic field of the tail is presented as a sum of two components: $\mathbf{B}_{\rm tail} = \mathbf{B}_1 + \mathbf{B}_2$. By this, $\mathbf{B}_2$, which provides the dominant contribution, is produced by the electric current in the tail current sheet. This current is closed via the tail magnetopause, and the component $\mathbf{B}_1$ is the curl-free field within the magnetosphere caused by the current closure.

In the parabolic coordinates (α, β, φ), associated with the dipole-centered PSM Cartesian coordinate system according to Equation (A2), the magnetic field of the tail current sheet is defined as the following (Belenkaya et al. 2005): $\mathbf{B}_2 = (B_{2\alpha}, 0, 0)$, where

$$B_{2\alpha} = B_{\rm t} \begin{cases} 0\,, & \alpha < \alpha_0 \\ \frac{f(\beta,\varphi)}{\alpha\sqrt{\alpha^2+\beta^2}}\,, & \alpha > \alpha_0\,. \end{cases} \tag{A4}$$

This field is divergence free everywhere except for the surface $\alpha = \alpha_0$, which intersects the x-axis (the stellar wind line) of the PSM Cartesian system down-tail at the point $(-R_2, 0, 0)$, corresponding to the inner boundary of the magnetotail current sheet. This enables us to write using the first expression in Equation (A2) that $R_2 = R_1(\alpha_0^2 - 1)/2$, and to define via the model parameters the constant $\alpha_0 = \sqrt{1 + 2R_2/R_1}$. The non-zero divergence of $\mathbf{B}_2$ on the surface $\alpha = \alpha_0$ is compensated by the curl-free field $\mathbf{B}_1$ so that the total field $\mathbf{B}_{\rm tail}$ satisfies the law: $\mathrm{div}\mathbf{B}_{\rm tail} = 0$.

The function $f(\beta, \varphi)$ in Equation (A4) determines the current profile in the magnetotail current sheet, which for simplicity is assumed to be a thin current sheet, e.g., $f(\beta,\varphi)=\mathrm{sign}((\pi/2)-|\varphi|)$. It may also be represented as a sum of Bessel function harmonics:

$$f(\beta, \varphi) = \sum_{n=1}^{\infty}\sum_{k=1}^{\infty} f_{\rm nk} J_{\rm n}(\lambda_{\rm nk}\beta)\cos[n\varphi]\ , \tag{A5}$$

where $\lambda_{\rm nk}$ are the zeros of $J'_{\rm n}(\lambda_{\rm nk})$, providing the zero normal component of the magnetic field at the magnetopause surface $\beta = 1$. To ensure the antisymmetry of the field relative to the current sheet in the equatorial plane, only the odd harmonics $n = 2m + 1 = 1, 3, 5, \ldots$ are considered in the sum in Equation (A5). The coefficients $f_{\rm nk}$ in Equation (11) are defined as $f_{\rm nk}=(4/\pi)((-1)^n/n)C_{\rm nk}$, where $C_{\rm nk}=N_{\rm nk}^{-1}\int_0^1 J_{\rm n}(\lambda_{\rm nk}\beta)\beta d\beta$ with the normalizing coefficient $N_{\rm nk}=1/2(1-(n^2/\lambda_{\rm nk}^2))J_{\rm n}^2(\lambda_{\rm nk})$ (for details see Belenkaya et al. 2005).

Since the normal component of the magnetic field turns to zero at the magnetopause surface $\beta = 1$, as well as at the magnetotail current sheet, the total magnetic flux in each lobe of the distant ($\alpha \to \infty$) tail magnetosphere is constant: $F_\infty = 0.5\pi R_1^2 B_{\rm t}$. This fact is used to express $B_{\rm t}$ in Equation (A4) via the model parameters: $B_{\rm t}=2F_\infty/\pi R_1^2$. Defined so, $B_{\rm t}$ also relates to the value of the cross-tail electric current. In the case of the solar system planets the value of the tail magnetic flux is usually determined from observations. For exoplanets such observations are impossible, and during the modeling we assumed the structure and magnetic flux partition in the magnetosphere of an exoplanet to be similar to those in the well-studied magnetospheres of solar system planets (e.g., Earth, Jupiter, and Saturn). In particular, following Alexeev & Bobrovnikov (1997), Alexeev et al. (2003), and Belenkaya et al. (2005), we supposed that the tail lobe magnetic flux, which determines the value of the tail current, is the same as the magnetic flux through the area limited by the inner edge of the tail current. In other words, the total tail magnetic flux is assumed to be shared in equal parts between the tail flux crossed by the equatorial plane and the tail lobe flux through the distant cross-section area perpendicular to the tail.

Finally, taking care of the continuity of the tail current magnetic field $\mathbf{B}_{\rm tail}$ at the surface $\alpha = \alpha_0$, Alexeev & Bobrovnikov (1997), Alexeev et al. (2003), and Belenkaya et al. (2005) provide the following expressions for its components in the parabolic coordinates:

$$\begin{aligned}
B_\alpha^{(\rm tail)}\big|_{\alpha<\alpha_0} &= -\frac{B_{\rm t}}{\sqrt{\alpha^2+\beta^2}}\sum_{n=1}^{\infty}\sum_{k=1}^{\infty} f_{\rm nk}\lambda_{\rm nk} K_{\rm n}(\lambda_{\rm nk}\alpha_0) J_{\rm n}(\lambda_{\rm nk}\beta) \\
&\quad \times I'_{\rm n}(\lambda_{\rm nk}\alpha)\cos[n\varphi], \\
B_\alpha^{(\rm tail)}\big|_{\alpha>\alpha_0} &= -\frac{B_{\rm t}}{\sqrt{\alpha^2+\beta^2}}\left(\frac{f(\beta,\varphi)}{\alpha} + \sum_{n=1}^{\infty}\sum_{k=1}^{\infty} f_{\rm nk}\lambda_{\rm nk}\right. \\
&\quad \left. \times I_{\rm n}(\lambda_{\rm nk}\alpha_0) J_{\rm n}(\lambda_{\rm nk}\beta) K'_{\rm n}(\lambda_{\rm nk}\alpha)\cos[n\varphi]\right), \\
B_\beta^{(\rm tail)}\big|_{\alpha<\alpha_0} &= -\frac{B_{\rm t}}{\sqrt{\alpha^2+\beta^2}}\sum_{n=1}^{\infty}\sum_{k=1}^{\infty} f_{\rm nk}\lambda_{\rm nk} K_{\rm n}(\lambda_{\rm nk}\alpha_0) \\
&\quad \times J'_{\rm n}(\lambda_{\rm nk}\beta) I_{\rm n}(\lambda_{\rm nk}\alpha)\cos[n\varphi], \\
B_\beta^{(\rm tail)}\big|_{\alpha>\alpha_0} &= -\frac{B_{\rm t}}{\sqrt{\alpha^2+\beta^2}}\sum_{n=1}^{\infty}\sum_{k=1}^{\infty} f_{\rm nk}\lambda_{\rm nk} I_{\rm n}(\lambda_{\rm nk}\alpha_0) \\
&\quad \times J'_{\rm n}(\lambda_{\rm nk}\beta) K_{\rm n}(\lambda_{\rm nk}\alpha)\cos[n\varphi], \\
B_\varphi^{(\rm tail)}\big|_{\alpha<\alpha_0} &= \frac{B_{\rm t}}{\alpha\beta}\sum_{n=1}^{\infty}\sum_{k=1}^{\infty} f_{\rm nk} n K_{\rm n}(\lambda_{\rm nk}\alpha_0) J_{\rm n}(\lambda_{\rm nk}\beta) \\
&\quad \times I_{\rm n}(\lambda_{\rm nk}\alpha)\sin[n\varphi], \\
B_\varphi^{(\rm tail)}\big|_{\alpha>\alpha_0} &= \frac{B_{\rm t}}{\alpha\beta}\sum_{n=1}^{\infty}\sum_{k=1}^{\infty} f_{\rm nk} n I_{\rm n}(\lambda_{\rm nk}\alpha_0) J_{\rm n}(\lambda_{\rm nk}\beta) \\
&\quad \times K_{\rm n}(\lambda_{\rm nk}\alpha)\sin[n\varphi].
\end{aligned} \tag{A6}$$

The n-summing in Equation (A6) is performed over odd terms only ($n = 1, 3, 5, \ldots$).

A.3. Screened Equatorial Magnetodisk

A simple model of a current-carrying plasma disk is included in the PMM (Alexeev & Belenkaya 2005) in order to reflect the main features of the magnetosphere with a magnetodisk: a slower-than-the-dipole-type ($\propto r^{-3}$) decrease of the magnetic field with the distance from a planet, and the quasi-radial direction of the magnetic field near the equatorial plane in the middle magnetosphere. Due to the axial symmetry of the object, the description of the magnetodisk fields deep inside the magnetosphere is performed in the spherical coordinate system (r, ϕ, θ) associated with the dipole-centered PSM Cartesian coordinate system, where the polar angle θ and azimuthal angle ϕ are counted from the parallel to the dipole z-axis and in the planet rotation direction, respectively.

The requirement of conservation of the magnetic flux above (and below) the disk surface supposes that the radial component of the magnetic field of the disk decreases as $\propto 1/r^2$, whereas $B_\theta \sim 0$ (due to high electroconductivity of the disk). Therefore, the surface density of the azimuthal electric current (i.e., the azimuthal current per unit radial distance) concentrated in the thin equatorial disk may be written as (Alexeev & Belenkaya

2005; Belenkaya et al. 2005)

$$i_\phi = \frac{2B_{\rm DC}}{\mu_0}\left(\frac{R_{\rm D1}}{r}\right)^2 , \qquad \text{(A7)}$$

where $B_{\rm DC}$ is the disk field at its outer edge ($r = R_{\rm D1}$). The magnetic moment of such disk current may be defined by the integration over the current distribution area (i.e., the thin disk) as the following (Landau & Lifshitz 1960):

$$\mathcal{M}_{\rm MD} = \pi \int_{R_{\rm D2}}^{R_{\rm D1}} i_\phi r^2 dr = \frac{4\pi}{\mu_0}\frac{B_{\rm DC}}{2} R_{\rm D1}^3 (1-\tilde{r}_0) , \qquad \text{(A8)}$$

where $\tilde{r}_0 = R_{\rm D2}/R_{\rm D1}$.

The model parameters in Equations (A7) and (A8) are determined by the planetary dipole magnetic flux above and below the equatorial disk. This flux corresponds to the dipole field lines which would cross, in the absence of the disk, the equatorial plane between the "Alfvénic surface" radius $R_{\rm A}$ and the outer edge of the disk $R_{\rm D1}$ (close to $R_{\rm s}$). Due to a very high (close to infinite) conductivity of the collisionless magnetodisk plasma, the magnetic flux above and below the disk is supposed to be conserved. The validity of this assumption has been demonstrated for the case of the solar system Jupiter by spacecraft in situ measurements (Alexeev & Belenkaya 2005; Alexeev et al. 2006). In particular, in the *Galileo* and *Ulysses* magnetometer data (e.g., Alexeev & Belenkaya 2005), the spacecraft crossing of the Jovian magnetodisk is recognized as a strong depression of the magnetic field, typical for a thin highly conducting current sheet. Near the disk, the spacecraft magnetometers show that the component of the magnetic field normal to the equatorial plane is about 10 times smaller than the radial one. This indicates a quasi-parallel to the equatorial plane direction of the magnetic field in the close vicinity of the disk. A similar picture is also observed in the case of Saturn (Arridge et al. 2008).

The detailed expressions for the components of the magnetic field generated by the disk have been obtained (Alexeev & Belenkaya 2005) in the following form:

$$\begin{aligned}
B_{\rm r}^{\rm (m.disk)}\big|_{r\geqslant R_{\rm D1}} &= B_{\rm DC}\sum_{k=0}^{\infty} a_{2k}(1-\tilde{r}_0^{2k+1})\frac{P_{2k+1}(\cos\theta)}{\tilde{r}^{2k+3}},\\
B_{\theta}^{\rm (m.disk)}\big|_{r\geqslant R_{\rm D1}} &= B_{\rm DC}\sum_{k=0}^{\infty} \frac{a_{2k}}{2k+2}(1-\tilde{r}_0^{2k})\frac{P_{2k+1}^1(\cos\theta)}{\tilde{r}^{2k+3}},\\
B_{\rm r}^{\rm (m.disk)}\big|_{R_{\rm D2}\leqslant r\leqslant R_{\rm D1}} &= B_{\rm DC}\Bigg[\sum_{k=0}^{\infty}\left(a_{2k+2}-\alpha_{2k}\frac{\tilde{r}_0^{2k+1}}{\tilde{r}^{4k+3}}\right)\\
&\quad\times \tilde{r}^{2k}P_{2k+1}(\cos\theta)+\frac{\mathrm{sign}(\cos\theta)}{\tilde{r}^2}\Bigg],\\
B_{\theta}^{\rm (m.disk)}\big|_{R_{\rm D2}\leqslant r\leqslant R_{\rm D1}} &= B_{\rm DC}\sum_{k=0}^{\infty} a_{2k}\left(\tilde{r}^{2k}-\frac{\tilde{r}_0^{2k+1}}{\tilde{r}^{2k+3}}\right)\frac{P_{2k+1}^1(\cos\theta)}{2k+2},\\
B_{\rm r}^{\rm (m.disk)}\big|_{r\leqslant R_{\rm D2}} &= B_{\rm DC}\sum_{k=0}^{\infty} a_{2k+2}\left(1-\frac{1}{\tilde{r}_0^{2k+2}}\right)\tilde{r}^{2k}P_{2k+1}(\cos\theta),\\
B_{\theta}^{\rm (m.disk)}\big|_{r\leqslant R_{\rm D2}} &= B_{\rm DC}\sum_{k=0}^{\infty} a_{2k}\left(\tilde{r}_0^{2k}-\frac{1}{\tilde{r}_0^{2}}\right)\frac{\tilde{r}^{2k}}{\tilde{r}_0^{2k}}\frac{P_{2k+1}^1(\cos\theta)}{2k+2},
\end{aligned} \qquad \text{(A9)}$$

where $P_{\rm n}(\cos\theta)$ and $P_{\rm n}^1(\cos\theta)$ are Legendre polynomials and associated Legendre polynomials, respectively, $\tilde{r} = r/R_{\rm D1}$ is dimensionless distance, and coefficient $a_{2k} = (-1)^k/2^k k!1\cdot 3\cdot 5\cdots(2k-1)$.

Since at large planetocentric distance the character of the magnetodisk field is similar to the dipole field, the corresponding magnetopause currents required to confine the magnetic field of the disk inside the magnetosphere may be defined in a way similar to the case of the screened magnetic dipole addressed above. By this, the parameter M_M defined by the planetary dipole $\mathcal{M}$ should be replaced in Equations (A1) and (A3) by $M_{\rm MD} = 2\mathcal{M}_{\rm MD}/R_1^2$ using Equation (A8).

REFERENCES

Achilleos, N., Guio, P., & Arridge, C. S. 2010, MNRAS, 401, 2349
Alekseev, I. I., Kropotkin, A. P., & Veselovskii, I. S. 1982, Sol. Phys., 79, 385
Alexeev, I. I. 1978, Geomagn. Aeron., 18, 656
Alexeev, I. I. 1986, J. Geomagn. Geoelectr., 38, 1199
Alexeev, I. I., & Belenkaya, E. S. 2005, Ann. Geophys., 23, 809
Alexeev, I. I., Belenkaya, E. S., Bobrovnikov, S. Yu., & Kalegaev, V. V. 2003, Space Sci. Rev., 107, 7
Alexeev, I. I., Belenkaya, E. S., Bobrovnikov, S. Yu., Slavin, J. A., & Sarantos, M. 2008, J. Geophys. Res., 113, A12210
Alexeev, I. I., Belenkaya, E. S., Slavin, J. A., et al. 2010, Icarus, 209, 23
Alexeev, I. I., & Bobrovnikov, S. Yu. 1997, Geomagn. Aeron., 37, 24
Alexeev, I. I., Kalegaev, V. V., Belenkaya, E. S., et al. 2006, Geophys. Res. Lett., 33, L08101
Alexeev, I. I., & Shabansky, V. P. 1972, Planet. Space Sci., 20, 117
Arridge, C. S., Russell, C. T., Khurana, K. K., et al. 2008, J. Geophys. Res., 113, A04214
Baraffe, I., Selsis, F., Chabrier, G., et al. 2004, A&A, 419, L13
Baumjohann, W., & Treumann, R. A. 1997, Basic Space Plasma Physics (London: Imperial College Press)
Belenkaya, E. S. 2004, Planet. Space Sci., 52, 499
Belenkaya, E. S. 2007, Geomagn. Aeron., 47, 33
Belenkaya, E. S. 2009, Phys.—Usp., 52, 765
Belenkaya, E. S., Alexeev, I. I., Blokhina, M. S., et al. 2007, Ann. Geophys., 25, 1215
Belenkaya, E. S., Alexeev, I. I., Kalegaev, V. V., & Blokhina, M. S. 2006, Ann. Geophys., 24, 1145
Belenkaya, E. S., Alexeev, I. I., Khodachenko, M. L., Panchenko, M., & Blokhina, M. 2010, in European Planetary Science Congress 2010 Abstracts, Stellar Wind Magnetic Field Influence on Exoplanet's Magnetosphere, 72, http://europlanet-jra3.oeaw.ac.at/fileadmin/presentations/EPSC2010/MG4/EPSC2010-72-1.pdf
Belenkaya, E. S., Bobrovnikov, S. Yu., Alexeev, I. I., Kalegaev, V. V., & Cowley, S. W. H. 2005, Planet. Space Sci., 53, 863
Belenkaya, E. S., Cowley, S. W. H., Badman, S. V., Blokhina, M. S., & Kalegaev, V. V. 2008, Ann. Geophys., 26, 159
Busse, F. H. 1976, Phys. Earth Planet. Inter., 12, 350
Caudal, G. 1986, J. Geophys. Res., 91, 4201
Chassefière, E. 1996, Icarus, 124, 537
Christensen, U. R. 2010, Space Sci. Rev., 152, 565
Christensen, U. R., & Aubert, J. 2006, Geophys. J. Int., 166, 97
Coroniti, F. V., & Kennel, C. F. 1977, Geophys. Res. Lett., 4, 211
Cowley, S. W. H., Alexeev, I. I., Belenkaya, E. S., et al. 2005, J. Geophys. Res., 110, A11209
Durand-Manterola, H. J. 2009, Planet. Space Sci., 57, 1405
Ekenbäck, A., Holmström, M., Wurz, P., et al. 2010, ApJ, 709, 670
Erkaev, N. V., Kulikov, Y. N., Lammer, H., et al. 2007, A&A, 472, 329
Erkaev, N. V., Penz, T., Lammer, H., et al. 2005, ApJS, 157, 396
Farrell, W. M., Desch, M. D., & Zarka, P. 1999, J. Geophys. Res., 104, 14025
García Muñoz, A. 2007, Planet. Space Sci., 55, 1426
Greene, J. M., & Miller, R. L. 1994, Planet. Space Sci., 42, 895
Grießmeier, J.-M., Preusse, S., Khodachenko, M. L., et al. 2007a, Planet. Space Sci., 55, 618
Grießmeier, J.-M., Stadelmann, A., Grenfell, J. L., Lammer, H., & Motschmann, U. 2009, Icarus, 199, 526
Grießmeier, J.-M., Stadelmann, A., Motschmann, U., et al. 2005, Astrobiology, 5, 587
Grießmeier, J.-M., Stadelmann, A., Penz, T., et al. 2004, A&A, 425, 753
Grießmeier, J.-M., Zarka, P., & Spreeuw, H. 2007b, A&A, 475, 359
Guinan, E. F., & Ribas, I. 2002, in ASP Conf. Proc. 269, The Evolving Sun and its Influence on Planetary Environments, ed. B. Montesinos, A. Gimenez, & E. F. Guinan (San Francisco, CA: ASP), 85
Holmström, M., Ekenbäck, A., Selsis, F., et al. 2008, Nature, 451, 970
Ip, W.-H., Kopp, A., & Hu, J.-H. 2004, ApJ, 602, L53
Johansson, E. P. G., Bagdonat, T., & Motschmann, U. 2009, A&A, 496, 869

Khodachenko, M. L., Lammer, H., Lichtenegger, H. I. M., et al. 2007a, Planet. Space Sci., 55, 631
Khodachenko, M. L., Ribas, I., Lammer, H., et al. 2007b, Astrobiology, 7, 167
Koskinen, T., Yelle, R. V., Lavvas, P., & Lewis, N. K. 2010, ApJ, 723, 116
Lammer, H., Kislyakova, K. G., Holmstroem, M., Khodachenko, M. L., & Grießmeier, J.-M. 2011, Ap&SS, 335, 9
Lammer, H., Lichtenegger, H., Kulikov, Yu., et al. 2007, Astrobiology, 7, 185
Lammer, H., Odert, P., Leitzinger, M., et al. 2009, A&A, 506, 399
Lammer, H., Selsis, F., Ribas, I., et al. 2003, ApJ, 598, L121
Landau, L. D., & Lifshitz, E. M. 1960, Electrodynamics of Continuous Media (Oxford: Pergamon)
Leitzinger, M., Odert, P., Lammer, H., et al. 2011, Planet. Space Sci., 59, 1472
Lipatov, A. S., Motschmann, U., Bagdonat, T., & Grießmeier, J.-M. 2005, Planet. Space Sci., 53, 423
Llama, J., Wood, K., Jardine, M., et al. 2011, MNRAS, 416, L41
Mann, G., Jansen, F., MacDowall, R. J., Kaiser, M. L., & Stone, R. G. 1999, A&A, 348, 614
Mestel, L. 1968, MNRAS, 138, 359
Mizutani, H., Yamamoto, T., & Fujimura, A. 1992, Adv. Space Res., 12, 265
Murray-Clay, R. A., Chiang, E. I., & Murray, N. 2009, ApJ, 693, 23
Newkirk, G., Jr. 1980, Geochim. Cosmochim. Acta Suppl., 13, 293
Parker, E. N. 1958, ApJ, 128, 664
Penz, T., Erkaev, N. V., Kulikov, Yu. N., et al. 2008, Planet. Space Sci., 56, 1260
Preibisch, T., & Feigelson, E. D. 2005, ApJS, 160, 390
Preusse, S., Kopp, A., Büchner, J., & Motschmann, U. 2005, A&A, 434, 1191
Preusse, S., Kopp, A., Büchner, J., & Motschmann, U. 2007, Planet. Space Sci., 55, 589
Reiners, A., & Christensen, U. R. 2010, A&A, 522, A13
Ribas, I., Guinan, E. F., Güdel, M., & Audard, M. 2005, ApJ, 622, 680
Russell, C. T. 1977, Geophys. Res. Lett., 4, 387
Sánchez-Lavega, A. 2004, ApJ, 609, L87
Sano, Y. 1993, J. Geomagn. Geoelectr., 45, 65
Showman, A. P., & Guillot, T. 2002, A&A, 385, 166
Slavin, J. A., Acuña, M. H., Anderson, B. J., et al. 2009, Science, 324, 606
Slavin, J. A., & Holzer, R. E. 1979, J. Geophys. Res., 84, 2076
Stevenson, D. J. 1983, Rep. Prog. Phys., 46, 555
Stevenson, D. J. 2003, Earth Planet. Sci. Lett., 208, 1
Tian, F., Toon, O. B., Pavlov, A. A., & De Sterck, H. 2005, ApJ, 621, 1049
Trammell, G. B., Arras, P., & Li, Z.-Y. 2011, ApJ, 728, 152
Vasyliunas, V. M. 1983, in Physics of the Jovian Magnetosphere, ed. A. J. Dessler (Cambridge: Cambridge Univ. Press), 395
Vidotto, A. A., Jardine, M., & Helling, C. 2011, MNRAS, 411, L46
Wood, B. E., Müller, H.-R., Zank, G. P., & Linsky, J. L. 2002, ApJ, 574, 412
Wood, B. E., Müller, H.-R., Zank, G. P., Linsky, J. L., & Redfield, S. 2005, ApJ, 628, L143
Yelle, R. V. 2004, Icarus, 170, 167
Yelle, R. V. 2006, Icarus, 183, 508
Zarka, P. 2007, Planet. Space Sci., 55, 598